1-9-2023

Dust and loess as archives and agents of climate and climate change in the late Paleozoic Earth system

Gerilyn S. Soreghan

Nicholas G. Heavens

Lily Pfeifer
Rowan University, pfeiferls@rowan.edu

Michael J. Soreghan

Recommended Citation

Soreghan Gerilyn S., Heavens Nicholas G., Pfeifer Lily S., & Soreghan Michael J. (2023) Dust and loess as archives and agents of climate and climate change in the late Paleozoic Earth system. Geological Society, London, Special Publications. 535(1), January 9, 2023, doi: 10.1144/SP535-2022-208.

Dust and loess as archives and agents of climate and climate change in the late Paleozoic Earth system

Gerilyn S. Soreghan[1]*, Nicholas G. Heavens[2], Lily S. Pfeifer[1,3] and Michael J. Soreghan[1]

[1]School of Geosciences, University of Oklahoma, 100 E. Boyd St, Norman, OK 73019, USA

[2]Space Science Institute, 4765 Walnut St, Suite B, Boulder, CO 80301, USA

[3]Department of Geology, Rowan University, 201 Mullica Hill Rd, Glassboro, NJ 08028, USA

GSS, 0000-0001-6925-5675
*Correspondence: lsoreg@ou.edu

Abstract: Palaeo-loess and silty aeolian-marine strata are well recognized across the Carboniferous–Permian of equatorial Pangaea. Aeolian-transported dust and loess appear in the Late Devonian in the west, are common by the Late Carboniferous, and predominate across equatorial Pangaea by the Permian. The thickest loess deposits in Earth history – in excess of 1000 m – date from this time, and archive unusually dusty equatorial conditions, especially compared to the dearth of equatorial dust in the Cenozoic. Loess archives a confluence of silt generation, aeolian emission and transport, and ultimate accumulation in dust traps that included ephemerally wet surfaces and epeiric seas. Orogenic belts sourced the silt, and mountain glaciation may have exacerbated voluminous silt production, but remains controversial. In western Pangaea, large rivers transported silt westward, and floodplain deflation supplied silt for loess and dust. Expansion of dust deposition in Late Pennsylvanian time records aridification that progressed across Pangaea, from west to east. Contemporaneous volcanism may have created acidic atmospheric conditions to enhance nutrient reactivity of dusts, affecting Earth's carbon cycle. The late Paleozoic was Earth's largest and most long-lived dust bowl, and this dust represents both an archive and agent of climate and climate change.

Supplementary material: Detrital zircon data not previously published are available at https://doi.org/10.6084/m9.figshare.c.6299508

A multitude of studies on the modern–recent have shown that atmospheric dust (mineral aerosols), including loess, both records and influences Earth's climate system in several ways. For example, it serves as a direct record of atmospheric circulation, and hydroclimate (e.g. Muhs *et al.* 2014). Furthermore, it both scatters and absorbs incoming solar and outgoing long-wave radiation and impacts Earth's energy balance locally and globally (e.g. Tegen *et al.* 1996; Di Biagio *et al.* 2020), which in turn affects atmospheric circulation (e.g. Mahowald *et al.* 2006; Yoshioka *et al.* 2007), and cloud formation (particularly of mixed-phase clouds; e.g. Rosenfeld *et al.* 2001; DeMott *et al.* 2003; Mahowald and Kiehl 2003; Tobo *et al.* 2019). Additionally, it supplies key, limiting nutrients – notably iron – to marine and terrestrial ecosystems that contribute to organic carbon cycling (e.g. Martin *et al.* 1991; Swap *et al.* 1992; Boyd *et al.* 2004; Jickells *et al.* 2005; Mahowald *et al.* 2005; Mahowald 2011) and promotes microbial activity that stimulates carbonate production (e.g. Bressac *et al.* 2014; Guieu *et al.* 2014; Swart *et al.* 2014).

Atmospheric mineral aerosols and dust deposits are increasingly well recognized in Earth's deep-time past, particularly from the Carboniferous–Permian, both as loess (continental aeolian silt) deposits, and as aeolian-transported silts ultimately captured in subaqueous environments, such as carbonate platforms and atolls, and swamps, lakes, and playas. Their prevalence in the Carboniferous–Permian record (e.g. Soreghan *et al.* 2008) – in deposits that exceed by more than an order of magnitude the thickest loess deposits recognized from the Quaternary (Soreghan *et al.* 2008; Pfeifer *et al.* 2021*a*) – signals a remarkably dusty atmosphere that likely influenced the late Paleozoic Earth system.

In this contribution, we review the geological record of dust from the late Paleozoic, with a focus on the western and eastern Pangaean equatorial region (Figs 1–3). Dust was sourced largely from erosion in the equatorial Central Pangaean Mountains (CPM), including auxiliary uplifts such as the Ancestral Rocky Mountains in the western USA, but secondarily from explosive equatorial volcanism

From: Lucas, S. G., DiMichele, W. A., Opluštil, S. and Wang, X. (eds) *Ice Ages, Climate Dynamics and Biotic Events: the Late Pennsylvanian World*. Geological Society, London, Special Publications, **535**,
https://doi.org/10.1144/SP535-2022-208

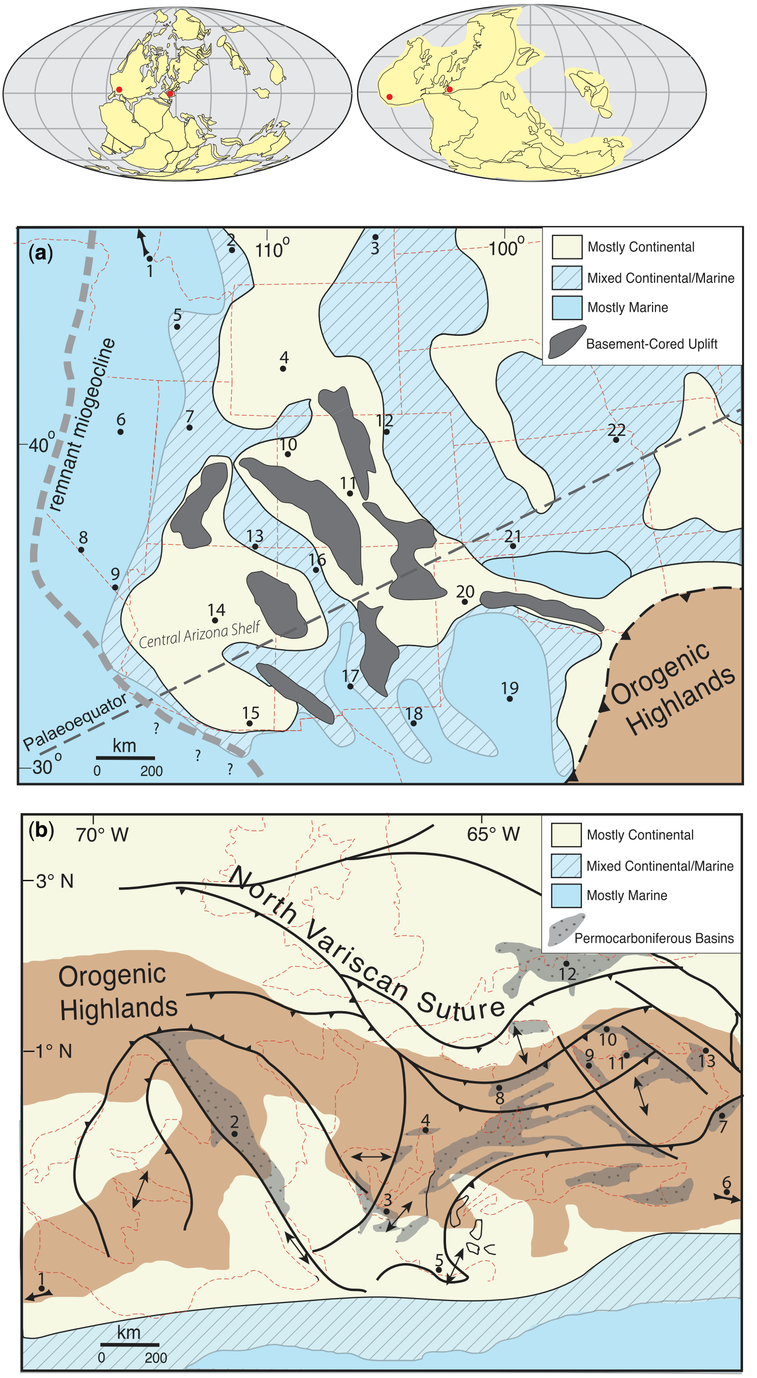

Fig. 1. Pangaea A (left) and B (right) configurations for the early Permian (*c.* 290 Ma). Red dots show the locations (generally) of the western USA and France (on either side of Pangaea). Maps show the locations of Permo-Carboniferous basins in western (a; present-day coordinates) and eastern (b; palaeogeographical coordinates) equatorial Pangaea. Numbers correspond with columns in Figures 2 and 3. Source: map of western USA is modified from Soreghan *et al.* (2008), and map of western Europe is modified from Matte (2001), Pochat and Van Den Driessche (2011), and Schneider and Lucas (2015).

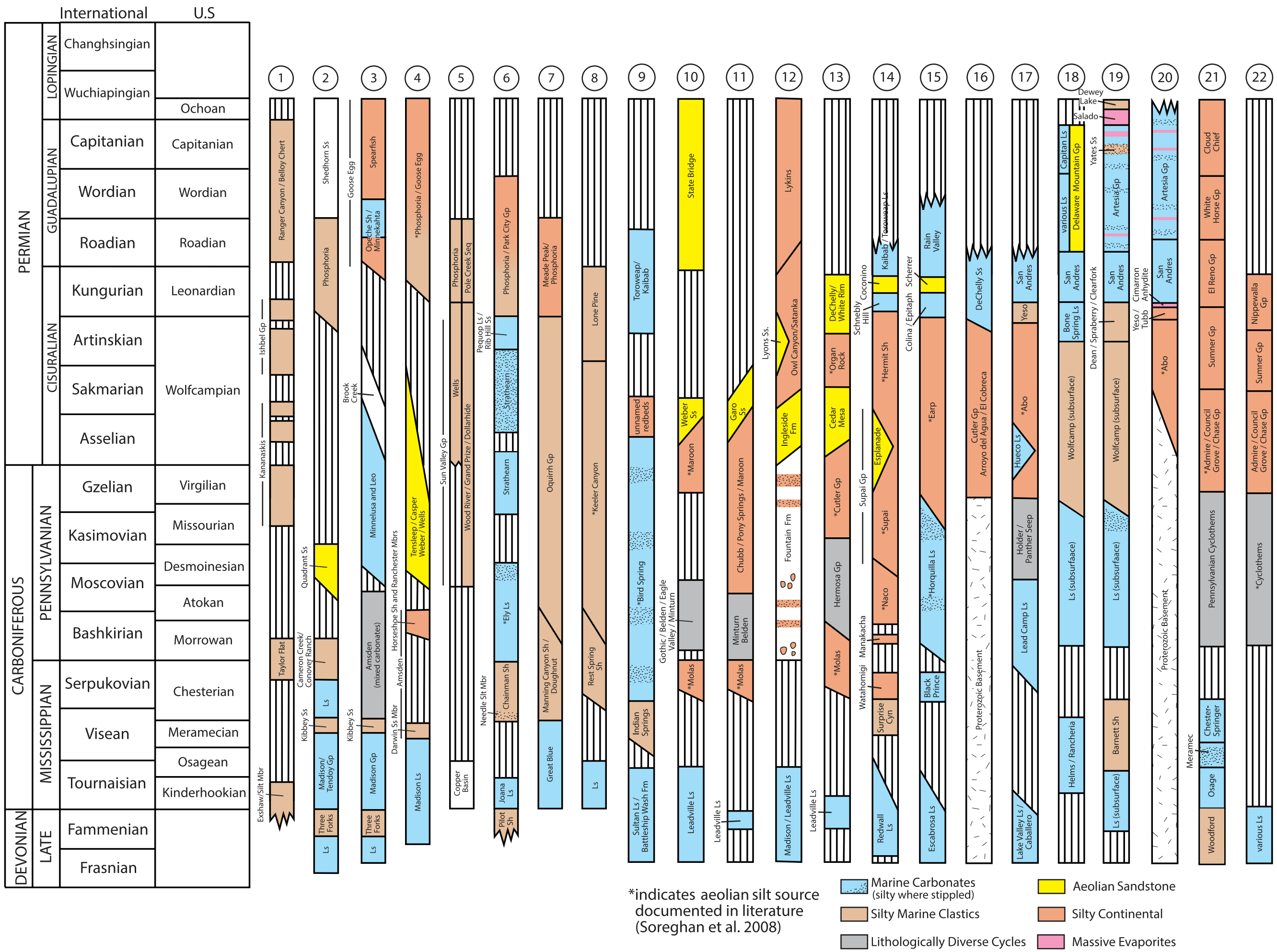

Fig. 2. Compilation of documented and hypothesized upper Paleozoic loess and dust in western equatorial Pangaea. Source: modified from Soreghan *et al.* (2008).

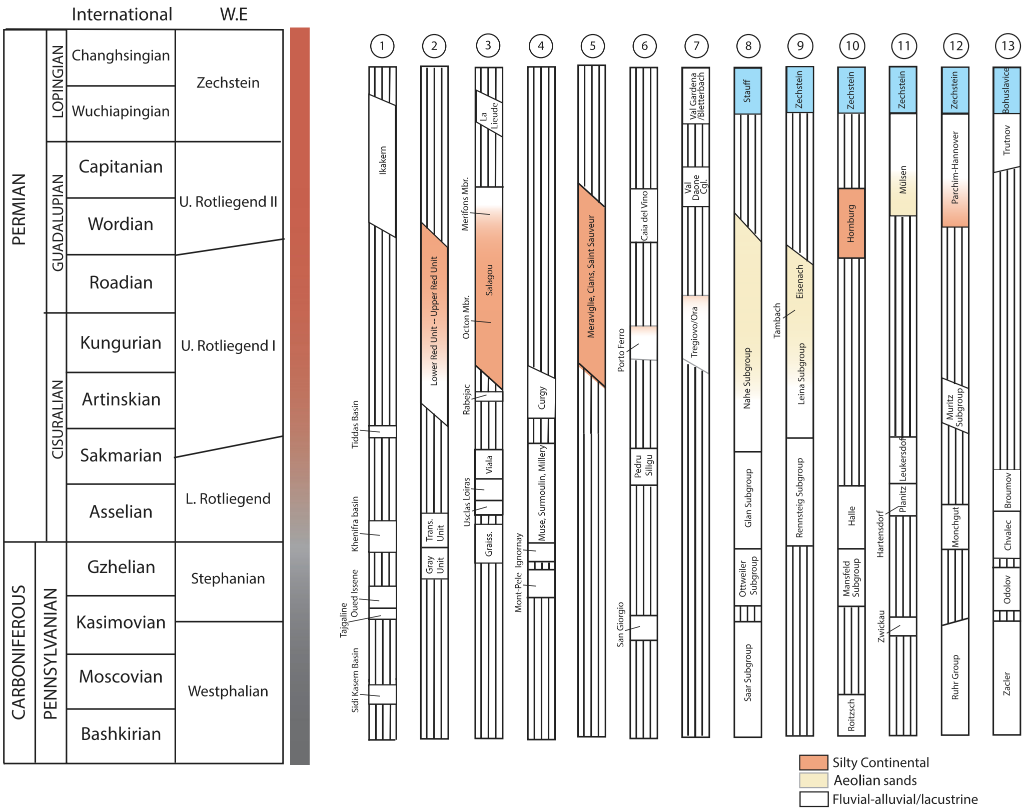

Fig. 3. Compilation of documented upper Paleozoic loess in eastern equatorial Pangaea (#3; Salagou Formation; Pfeifer *et al.* 2021*a*) and correlative units in continental basins within the European Variscan belt. Compilations from Schneider *et al.* (2006, 2014, 2019 and references within) have been modified to include tentative interpretations (colour) about continental silt-rich units that may represent loess deposition (interpreted from stratigraphic descriptions in the literature; Geluk 1958; Vinchon 1984; Breitkreuz *et al.* 2009; Voigt *et al.* 2010; Pochat and Van Den Driessche 2011; Schäfer 2012; Cassinis *et al.* 2012; Lagnaoui *et al.* 2014; Marchetti *et al.* 2015; Opluštil *et al.* 2016; Mujal *et al.* 2018; Buchwitz *et al.* 2020; Pfeifer *et al.* 2021*b*; Mercuzot *et al.* 2022).

that increased in abundance from Carboniferous into Permian time, especially in western Europe. We demonstrate that atmospheric dust loading became increasingly important in the late Paleozoic Earth system, especially as Pangaea aridified, with substantial implications for Earth's biosphere.

Definition of loess and dust

'Dust' can be defined simply as a suspension of solid particles in a gas (Pye 1987; Muhs 2013), as well as referring to deposits of such material (Muhs 2013). Although dust can refer colloquially to both loess and (fine) dust, Stuut *et al.* (2009) emphasized the importance of distinguishing between loess and dust, or 'large dust and small dust' (cf. Livingstone and Warren 1996). In their definition, large dust is silt in the 16–63 µm range, and is the material commonly composing loess deposits, whereas small dust is typically <10 µm – material that can be transported for long, even global, distances (Tsoar and Pye 1987), commonly referred to as long-range transported (LRT) dust (Muhs *et al.* 2014).

In its simplest definition, 'loess' refers to continental deposits of windblown silt, composed primarily of quartz, feldspars, and phyllosilicates (e.g. Pye 1995; Muhs and Bettis 2003). Owing to a focus in the loess literature on the relatively recent geological record, and the common association of loess with soils, the silt size mode is typically taken as ranging from 2 to 63 µm by Quaternary geologists and soil scientists (e.g. Stuut *et al.* 2009; Muhs *et al.* 2014), but sedimentologists consider silt to range from 4 to 63 µm (Wentworth 1922; Blott and Pye 2012). Several authors have suggested the existence of a 'loess mode' in the range of 20–30 µm (Assallay *et al.* 1998) or 20–40 µm (Tsoar and Pye 1987) or 20–50 µm (Smalley and Krinsley 1978), although loess commonly contains material both smaller and larger that these proposed 'typical' modes (Muhs 2013). Pye (1995) noted that there is no single loess 'mode' given that model size hinges on factors such as transport distance (cf. Chinese Loess; Porter 2001). Muhs *et al.* (2014) noted that 60–90% of loess consists of silt-sized particles, with minor sand and clay.

Owing to the small particle sizes, dust travels via suspension rather than saltation, with coarser dust (*c.* 20–70 µm) carried in short-term suspension and generally deposited relatively proximal to the source, and finer dust (<20 µm) carried in LRT, and deposited thousands of (or more) kilometres from the source (Pye 1987; Muhs 2013). Total transport distance can be complicated by intermediate river transport, however, especially given the importance of rivers to loess accumulations (Smalley *et al.* 2009), such that coarser silt can travel hundreds or more kilometres in rivers prior to aeolian emission from floodplains (e.g. Li *et al.* 2020). Exceptions to particle size generalizations include so-called giant grains now documented in both modern and deep-time dusts, that clearly travelled anomalously far from their source(s) owing to various atmospheric transport mechanisms (e.g. Betzer *et al.* 1988; Stuut *et al.* 2005; Van der Does *et al*. 2018). Climate models often focus on the fraction *c.* 10 µm and finer, as this size range is the most significant for long-range transport, effects on radiative forcing, and fueling nutrient release (Mahowald *et al.* 2006, 2011; Albani *et al.* 2014, 2015).

The conditions necessary to form a dust or loess deposit include (Pye 1995) the need for (1) (a) silt source(s), (2) the capacity for dust emission – meaning both adequate wind energy and some amount of aridity in the deflation region (e.g. dry floodplains and playas), (3) transport via both the atmosphere and rivers, and finally (4) a site suitable for accumulation. A component of fluvial transport seems important for many systems, with much loess (deflating from and) accumulating within a few tens of kilometres of river channels and floodplains (e.g. Smalley *et al.* 2009; Fenn *et al.* 2022), albeit the finest fraction can travel much farther. Dust accumulation on land (as loess) is aided by accumulation in the lee of barriers to saltating sand transport, such as river valleys and escarpments (Mason *et al.* 1999), and by trapping caused by plants and surface moisture – such that semi-aridity is better than hyperaridity for accumulation (e.g. Tsoar and Pye 1987; Pye 1995). Aeolian-transported material can also be trapped in water bodies, including lakes and seas, where it is sometimes termed 'aeolian-marine' deposits (e.g. Radczewski 1955; Fischer and Sarnthein 1988; Soreghan 1992; Carroll *et al.* 1998; Rea 2009). For the case of Quaternary loess, some infer a post-depositional process of 'loessification' wherein meshes of needle-like calcite form between grains, trapping infiltrated clays (Smalley and Marković 2014) and influencing collapsibility.

The question of source continues to be hotly debated in the loess literature, as the manufacturing of large volumes of silt is not as straightforward as it might seem. Consider the case of chemical weathering of a granitoid: one is left with predominantly sand and gravel (Blatt 1967; Chiu and Ng 2014), implying the need for physical weathering to produce silt-sized grains in the case of silt-poor parent rocks. The predominance of loess in Earth's recent (late Cenozoic, especially Pleistocene) record, and its common occurrence in mid- to high-latitude regions close to the margins of former ice sheets, have led to an oft-cited connection between loess and glaciation, and recognition of the importance of glacial grinding for the ready production of voluminous silt (e.g. Smalley 1966, 1995; Smalley *et al.* 2001; Muhs and Bettis 2003; Li *et al.* 2020). The capacity for glacial grinding to crush primary silicates to silt sizes is unequivocal, but occurrences of loess and loess-like deposits linked by provenance to volcanigenic processes, or that occur in or near warm desert environments call for nonglacial mechanisms that must also be viable for silt production. These include reworking (physical erosion) of silt-rich precursors such as mud- or siltstone, volcanic ash, or phyllite, for example. Indeed, loess in some regions is dominated by volcanic input (e.g. South America – Zárate 2003; Alaska – Muhs *et al.* 2004; Japan – Matsu'ura *et al.* 2011; North America – Mason 2001; Aleinikoff *et al.* 2008; Yang *et al.* 2017). Loess associated with warm deserts tends to be either finer or coarser than the 'typical' loess mode cited above. For example, loess exhibiting bimodal particle-size distributions (3–8 µm and 50–60 µm) in the Negev Desert of Israel was transported and sorted (through the dunes of Sinai–Negev) from the lowstand-exposed Mediterranean shelf (Crouvi *et al.* 2008, 2010; Ben-Israel *et al.* 2015). The largest source of dust today emanates from the Bodélé Depression – a desert region of former lake Megachad (Washington *et al.* 2003, 2006; Bristow *et al.* 2009; Stuut *et al.* 2009) that sources dust to the Canary Islands – with modes of *c.* 5 µm and diatomaceous compositions (Stuut *et al.* 2009; citing data in Coudé-Gassen 1987; Torres-Padrón *et al.* 2002; Menéndez *et al.* 2007). Although some have argued for the efficacy of silt production by processes such as aeolian sand saltation and associated intergranular collisions (e.g. Whalley *et al.* 1987; Smith and Lowe 1991;

Wright *et al.* 1998; Wright 2001; Bullard *et al.* 2004, 2007; Enzel *et al.* 2010), experiments using realistic wind velocities, as well as empirical observations support only a negligible role for these processes (Kuenen 1960; Swet *et al.* 2019; Adams and Soreghan 2020). However, debate continues over the relative efficacy of many non-glacial mechanisms to generate silt, including fluvial comminution, chemical weathering, and frost- and salt weathering, for example (e.g. review in Fenn *et al.* 2022).

The utility of dust and loess

Loess is comparable to lacustrine and oceanic sediment in its capacity to record continuous or near-continuous deposition; furthermore, it is deposited directly from the atmosphere. Accordingly, like lake deposits, loess captures high-resolution (millennial-scale) archives of climate and environmental conditions on land (Beget and Hawkins 1989). For dust and loess, bulk geochemistry as well as rock magnetism provide weathering and provenance information (Soreghan and Soreghan 2007; Buggle *et al.* 2011; Maher 2011, 2016; Obreht *et al.* 2019), while composition, grain size, and grain morphology (shape) have important implications for radiative forcing, with dust capable of imposing either a cooling or warming effect (e.g. Mahowald *et al.* 2006, 2014; Balkanski *et al.* 2007; Durant *et al.* 2009; Atkinson *et al.* 2013; Di Biagio *et al.* 2020). Particle size distribution (PSD) can be particularly useful, especially when combined with other metrics, for interpretation of, for example, hydroclimate, dust loading, storm activity (Újvári *et al.* 2016), and other palaeoenvironmental data. With the advent of laser particle size analysis (LPSA), various algorithms have been proposed for decomposition of multimodal PSDs to extract further detail from these datasets (e.g. Liu *et al.* 2021). Magnetic susceptibility and frequency dependency of susceptibility provide baseline data on climate, pedogenesis, and/or possible diagenetic effects, owing to formation or dissolution of iron minerals (e.g. Forster *et al.* 1994; G.S. Soreghan *et al.* 1997; Maher 2011, 2016; Buggle *et al.* 2014; M.J. Soreghan *et al.* 2014; Pfeifer *et al.* 2020). Quantitative colour (spectrophotometry) of loess can reflect parameters such as magnetic minerals, thus providing a proxy for magnetic susceptibility and palaeoenvironmental conditions (e.g. Ji *et al.* 2001; Sprafke *et al.* 2020). Anisotropy of magnetic susceptibility – carefully interpreted – can reveal insight on palaeo-wind, and environments (e.g. pedogenically altered, bioturbated, subaerial v. subaqueous deposition; Tarling and Hrouda 1993; Zhu *et al.* 2004; Nawrocki *et al.* 2006; Zeeden *et al.* 2015; Bradák *et al.* 2020). And anhysteretic and isothermal remanent magnetization (ARM, IRM) provide information on magnetic grain size and concentration, which, combined with magnetic susceptibility, can yield information on transport and provenance (Buggle *et al.* 2014). These and various metrics can be used to evaluate astronomical forcing (cyclicity), for example, in the use of PSD and magnetic susceptibility variations to construct orbital age models (e.g. Heslop *et al.* 2000; Basarin *et al.* 2014). Additionally, detrital zircon geochronology – a well-established approach to provenance – was first applied to (palaeo)loess deposits by Soreghan *et al.* (2002) to inform loess transport pathways, including reconstruction of atmospheric circulation. It has subsequently been applied widely in both Quaternary loess (e.g. Aleinikoff *et al.* 2008; Stevens *et al.* 2010; Dendy *et al.* 2021; Fenn *et al.* 2022) and deep-time loess/aeolian-marine dust (e.g. Sweet *et al.* 2013; Foster *et al.* 2014; Pfeifer *et al.* 2018; Soreghan *et al.* 2018; McGlannan *et al.* 2022).

Recognition of dust in Earth's deep-time record

To a large degree, the same approaches used to identify loess and dust (or contributions thereof) in recent and Plio-Pleistocene sediment are applicable to deep-time systems (see Soreghan *et al.* 2008, 2022). The primary difference is the common lithification into mudstone and siltstone for deep-time units. In both near- and deep time, loess is recognized as silt dominated, with varying modes within the silt fraction, and the potential inclusion of both clay- and fine sand-sized material (Pye 1995; Soreghan *et al.* 2008; Muhs *et al.* 2014). Because dust settles out of suspension, loess deposits are typically internally massive, lacking sedimentary structures, and creating 'beds' up to several metres thick. Dust deposition competes constantly with plant colonization, so that loess and (post-Silurian) palaeoloess deposits commonly contain pedogenically altered horizons that record prolonged intervals of less-arid, less-dusty times; these palaeosols typically form the primary bedding in loess deposits. Dust blankets the land, so that loess deposits are laterally extensive, and typically lack evidence of the channelling, grading, or basal erosion commonly associated with fluvial and floodplain deposits.

By definition, loess and palaeo-loess accumulate on land, but aeolian-transported fines settle into every environment, including, for example, marine, lacustrine, glacial, and transitional/fluvial systems (references above), where recognition of their origin can be more challenging. Inferring an aeolian dust origin for detrital siliciclastic material in these settings requires – in addition to examination of the sedimentology – sufficient knowledge of transport processes to enable elimination of all but aeolian delivery. For example, Sur *et al.* (2010) used the palaeogeographical setting of isolated carbonate buildups of the so-called 'Horseshoe Atoll' in the subsurface of the Midland Basin (west Texas) to establish an aeolian transport model for siliciclastic fines. In this otherwise entirely carbonate setting, thin, clearly marine mudrock marked the sequence boundaries recording glacial lowstand and incipient transgressive intervals. But palimpsest pedogenic features recorded initial deposition of the mud as loess, that was subsequently drowned and overprinted during glacial-to-interglacial transitions. Similarly, siliciclastic fractions interpreted to represent aeolian-transported dust contributions occur in the Akiyoshi atoll of Japan (Qi 2016) – thousands of kilometres from potential dust sources – as well as in carbonate platform systems studied from sites in western equatorial Pangaea (e.g. Soreghan 1992), and in palaeo-mid-latitudes of the northern and southern hemispheres (e.g. Bolivia, Iran, Svalbard; Carvajal *et al.* 2018; Oordt *et al.* 2020; Sardar Abadi *et al.* 2020).

Although an aeolian transport and delivery model can be argued with high confidence in cases such as a core derived from a system for which no up-slope siliciclastic sources exist (e.g. a carbonate system or a continental ice cap), an aeolian origin is murkier in the case of units deposited in siliciclastic marine and lacustrine systems. In near-time systems, reasonable inferences of a dust origin have been established for, for example, deep-sea cores situated far from deltaic or submarine fan delivery systems (e.g. Pacific – Rea *et al.* 1985; Stuut *et al.* 2009), or lacustrine cores from lakes receiving quasi-continuous dust input (e.g. Biwa – Yamada 2004). Dust is also a very well-recognized component of modern soils – especially in arid regions (e.g. Yaalon and Ganor 1973; Reheis *et al.* 1995) – identifiable in part by a composition that demonstrates allochthonous input (e.g. Mason and Jacobs 1998). A composition grossly inconsistent with the substrate also signals allochthonous dust input, for example, quartzose contributions to basaltic volcanic oceanic island systems (cf. Hawaii example; Muhs *et al.* 1990; Muhs 2013) or high clastic-carbonate contributions to otherwise organic-rich lacustrine systems (cf. maar lakes; Dietrich and Seelos 2010). In these cases, the attributes enabling interpretation of a dust influence are particle-size characteristics (silt and finer) consistent with aeolian transport, together with geographical circumstances that enable elimination of fluvial or deltaic (or submarine fan) transport or nepheloid layers, and/or mineralogical or geochemical evidence for allochthonous input. Similarly, dust is incorporated into peats, where it will ultimately become part of the coal ash (coal-combustion residuals – see below; e.g. Steinmann and Shotyk 1997; De Vleeschouwer *et al.* 2012; Large and Marshall 2015; Sjöström *et al.* 2020; Large *et al.* 2021).

Analogous arguments are made for inferences of aeolian silt transport for deep-time systems. For example, Fischer and Sarnthein (1988) pointed to the now well-recognized aeolian sediment transport into marine systems occurring off the coast of the western Sahara as an analogue for the relatively well-sorted (fine) sandstone and siltstone that predominate in deep-water systems of the Permian Delaware Basin of West Texas; indeed, an aeolian transport model for these units had been raised by previous authors as early as the 1950s (Newell *et al.* 1953; Hull 1957; Harms 1974). Subsequently, aeolian transport for anomalously silt-rich strata have been widely recognized in deep-time units, especially for strata from the Carboniferous–Permian (see summary in Soreghan *et al.* 2008, and Figs 2 & 3). More recently, an aeolian-transport but marine deposition model has been invoked for units as old as the late Ordovician (Soom Shale, South Africa; Gabbott *et al.* 2010), Late Devonian (Woodford Shale, USA; McGlannan *et al.* 2022), and the Mississippian Sycamore and Meramecian units of the US mid-continent (McGlannan *et al.* 2022). The Devono-Mississippian interpretations are based on the diagnostically detrital (rather than authigenic or biogenic) origin of the silt-sized fraction of the siliciclastic contribution, laterally extensive facies distribution, and palaeogeographical setting in the sub-tropical arid belt, far from the nearest possible fluvio-deltaic feeder systems (McGlannan *et al.* 2022). Dust delivery has even been inferred for units bearing clear signs of fluvial deposition but composed entirely of silt-sized sediment – notably the Permian Abo Formation – which Mack *et al.* (2003) analogized to the Huang He River that drains through the Chinese Loess Plateau.

Records of upper Paleozoic dust (equatorial Pangaea)

Dust deposits of western equatorial Pangaea (Western-Midcontinental USA)

Within western equatorial Pangaea, the middle–late Paleozoic marks a transition from relative tectonic quiescence (Cambrian–Devonian; e.g. Yonkee *et al.* 2014; Scotese 2021) accompanied by carbonate deposition in epeiric seas, to widespread orogenesis along the western/southwestern, eastern, and southern margins of the North American craton (present-day coordinates; Fig. 1). Along the west, the early Mississippian Antler orogeny occurred – an arc-continent or perhaps Mediterranean-type thrust belt (Speed and Sleep 1982; Burchfiel and Royden 1991). In contrast, the ESE involved the progressive collisions and orogenic episodes ultimately culminating in the Central Pangaean Mountains, including the Appalachian (Acadian–Alleghanian) and Ouachita–Marathon systems (uplifts and adjacent forelands) extending from the NE (Atlantic Canada) to the SW (southwestern USA), and contiguous orogenic systems in Europe (Lawton *et al.* 2021; Scotese 2021; see below). The Ancestral Rocky Mountains contrasted greatly with these plate-boundary orogenic systems largely characterized by thrust belts and adjacent foreland basins reflecting the equator-parallel suturing of Gondwana and Laurentia to form Pangaea. Instead, the Ancestral Rocky Mountains formed across a broad SE–NW-trending swath of Laurentia, from Oklahoma to Wyoming and consisted of intraplate, basement-involved block uplifts and adjoining basins (e.g. Kluth and Coney 1981; Ye *et al.* 1996). The history of early Paleozoic carbonate deposition followed by later Paleozoic collisional tectonics makes detrital zircon geochronology an especially useful tool for reconstructing Carboniferous–Permian sediment transport pathways. Many of the silt-rich units of this region lie preserved in the basins of the Ancestral Rocky Mountains system, especially given that erosion of the palaeo-piedmont of the Appalachian system

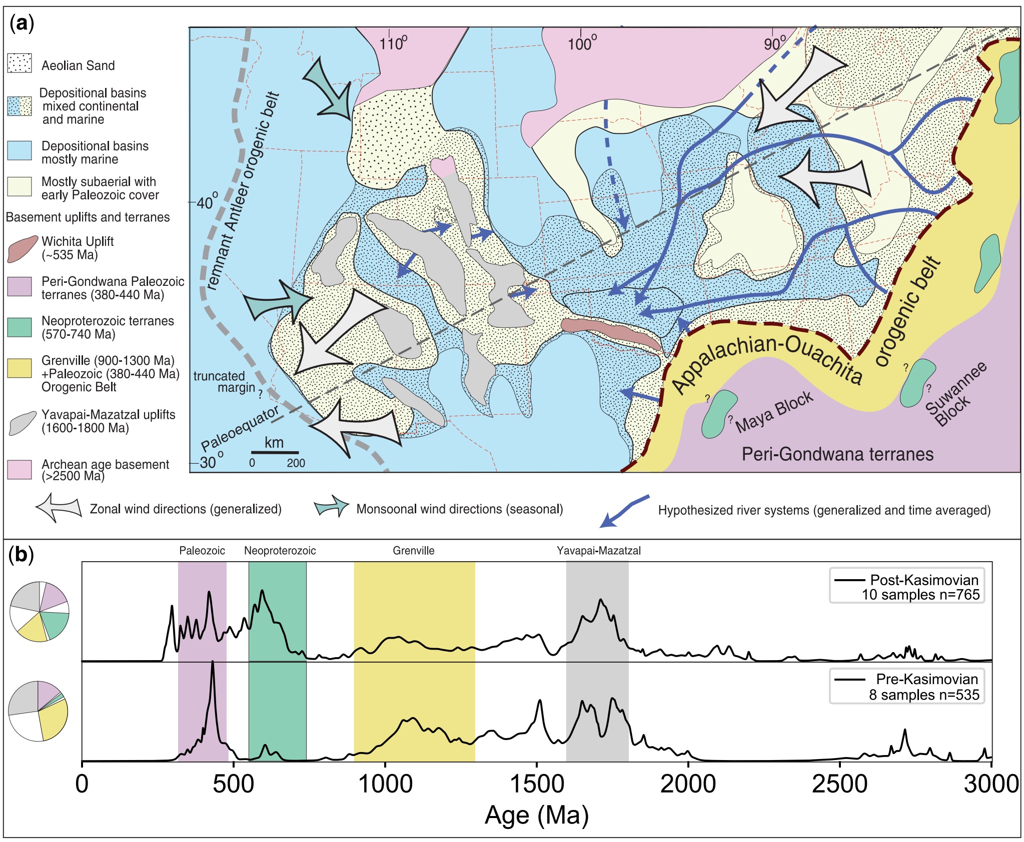

Fig. 4. Provenance and palaeogeography of western equatorial Pangaea. (**a**) Palaeogeographical map displaying depositional and uplifted regions. Note the palaeogeography is mainly reflective of the Kasimovian, but is necessarily time-averaged as it incorporates high-frequency glacioeustasy as well as long-term regression. Wind directions are idealized for both zonal (pre-Kasimovian) and monsoonal (post-Kasimovian) atmospheric circulation. Rivers (blue arrows) are idealized from Kushner *et al.* (2022), Lawton *et al.* (2021) and Thomas *et al.* (2020) and reflect drainage patterns extant; these river systems were not active simultaneously, nor throughout the entire time period. Basement ages of uplifts, terranes, and orogenic belt are from Soreghan *et al.* (2018), Lawton *et al.* (2021), and Alsalem *et al.* (2021). (**b**) Detrital zircon age spectra for compiled palaeo-loess and silty marine carbonates (data sources available in the supplementary data). The data are divided into pre-Kasimovian and Kasimovian (lower panel) and post-Kasimovian (upper panel). Coloured bars in the probability plot and coloured slices of the pie charts are colour coded the same as the uplift and terranes in part (a). Source: (a) modified from Kushner *et al.* (2022) and Soreghan *et al.* (2018).

essentially removed most of the Permian record of North America east of the mid-continent region.

Marine carbonate strata predominate in the upper Devonian to Carboniferous of western-midcontinent North America, but sporadic marine 'shale' and silty carbonate units occur, with unclear origins. The origins are unclear because they contain substantial amounts of siliciclastic material in the (predominantly) silt size fraction, but with no evidence of proximal fluvial-deltaic feeder systems to have transported this material to ultimate deposition in the marine system. Owing in part to this perplexing association, Soreghan *et al.* (2008) suggested that many of these are aeolian-marine units, fed by winds and sourced by the erosion of growing orogenic belts of the (primarily) Appalachian and Ouachita systems. More recently, McGlannan *et al.* (2022) amassed various data to explicitly posit aeolian origins for several enigmatic shaley and silty units of the Late Devonian–Mississippian that punctuate the otherwise carbonate-dominated stratigraphy of this middle– to early–late Paleozoic interval within the US mid-continent (Oklahoma). For example, the Upper Devonian Woodford Shale (Oklahoma), and (Fammenian) correlatives occur across the greater region, from the NW (e.g. Exshaw and Three Forks of Montana) to the ESE (e.g. Ohio and Chattanooga shales of Kentucky and Tennessee; McGlannan *et al.* 2022). Throughout the Lower Carboniferous, silty to cherty intervals punctuate carbonates of the midcontinent to eastern USA, increasingly ascribed to aeolian delivery of siliciclastic material (e.g. Soreghan *et al.* 2008; Cecil *et al.* 2018; McGlannan *et al.* 2022).

By Late Carboniferous (Pennsylvanian) time, the evolving palaeogeography of the western-midcontinent region appears to have set the stage for the appearance of continental aeolian deposits. The harbinger of this shift is the Molas Formation, a red siltstone of Bashkirian (Early Pennsylvanian) age that occurs at the unconformable contact between the Mississippian Leadville Limestone and overlying Carboniferous strata. This siltstone is interpreted as loess that was trapped and incorporated into the palaeokarst formed atop the Leadville Limestone (Evans and Reed 2007). The detrital zircons in the Molas Formation are dominated by Grenville (1300–900 Ma) and Paleozoic (440–380 Ma) U–Pb ages that reflect transportation from peri-Gondwanan terranes and the Appalachian–Ouachita orogenic system (Fig. 4a), *c.* 2000 km distant (Evans and Soreghan 2015), and appears to be the first true loess deposit of the late Paleozoic in western equatorial Pangaea. Interestingly, there are few U–Pb ages in the Molas Formation that reflect the local basement-cored uplifts dominated by Yavapai–Mazatzal age rocks (1800–1600 Ma) within the Ancestral Rocky Mountains (Fig. 4a; Evans and Soreghan 2015). However, by Late Carboniferous (Moscovian) time, loess deposits were widespread in and around the core of the Ancestral Rocky Mountains (ARM) uplifts of modern-day Colorado and northeastern Arizona, and detrital zircons in these strata exhibit U–Pb ages that match the local basement-cored uplifts, with Yavapai–Mazatzal basement ages, as well as zircons matching the peri-Gondwanan terranes and Appalachian–Ouachita orogenic belt (Fig. 4b – pre-Kasimovian). The increase in loess deposits likely reflects in part the growing prominence of this intraplate orogenic system (Fig. 4a), and perhaps the dust-trapping capacity of the ensuing topographic relief, although zircons in these strata also indicate derivation from the distal Appalachian–Ouachita orogen and peri-Gondwanan terranes. In regions a bit farther from the core ARM, anomalous siliciclastic silt appears in epeiric-sea carbonate strata – for example within the Moscovian (Middle Pennsylvanian) and later Ely and Bird Springs limestones (Nevada), to the Horquilla Limestone of southern Arizona (Soreghan *et al.* 2008) – analogous to its occurrences in Lower Carboniferous limestones that, like their continental counterparts, suggest both local (ARM uplifts) and distal (Appalachian–Ouachita orogen) sources.

In contrast to the pre-Kasimovian (Late Pennsylvanian) interval, the post-Kasimovian comprises widespread and well-documented palaeo-loess deposits, in addition to a continuation of the marine-deposited aeolian silt well recognized in many parts of western equatorial Pangaea (Fig. 2). Following the initial appearance of loess deposits first in regions within and surrounding the core Ancestral Rocky Mountains, loess began to predominate across the greater region. By the Carboniferous–Permian boundary, great thicknesses of silt- and mudstone interpreted as palaeo-loess prevail from the SW (Grand Canyon) to the mid-continent (Oklahoma–Kansas), and inferred aeolian-marine siltstone units populate regions inboard of the remnant Antler orogenic margin (Fig. 4a). The detrital zircon signature of these deposits shows subtle differences from older (pre-Kasimovian) dust deposits (Fig. 4b) that reflect evolution of the orogenic system as well as palaeogeography, including the development of trans-continental fluvial systems (Fig. 4a). Although zircons with ages matching the Yavapai–Mazatzal terranes (1800–1600 Ma) are present, particularly in palaeo-loess within and adjacent to the ARM (e.g. Maroon Formation and Cutler Group (Fig. 2; Soreghan *et al.* 2002, 2014)), this age grouping becomes less prominent over time, although locally important in upper Carboniferous–lower Permian strata as monsoonal (westerly) winds directed dust transport back eastward (Soreghan *et al.* 2002, 2014). For palaeo-loess in the Mid-Continent region (Oklahoma, Kansas, eastern New Mexico), U–Pb ages are dominated by Grenville (1300–900 Ma) and Paleozoic (3800–440 Ma) ages, reflecting far-travelled silt likely aided by transport in river systems prior to deflation. But these deposits also contain zircons with younger Paleozoic ages as well as Neoproterozoic ages (740–570 Ma; Fig. 4b), suggesting that rivers began tapping different terranes juxtaposed within the orogenic system. From the Asselian (early Permian) onward, loess predominates in the stratigraphic record across many parts of the western and midcontinental USA

It has long been known that assembly and breakup of supercontinents impacts sea level, via effects related to both seafloor age, and dynamic topography (e.g. Hallam 1984; Haq and Schutter 2008; Young *et al.* 2022). Both observations and modelling indicate that the hypsography of Pangaea evolved such that – on the first-order scale – sea levels generally fell from Late Devonian through Permian time (Young *et al.* 2022), reflected in the increasingly common occurrence of continental facies in the later Carboniferous and Permian across equatorial Pangaea. From this perspective, the long-term shift in western equatorial Pangaea from largely aeolian-marine units in the pre-Kasimovian, to increasingly aeolian-continental (loess, as well as aeolian sandstone) strata in the post-Kasimovian is perhaps unsurprising. However, independent of the shift in ultimate depositional setting, this shift records a significant increase in the sheer volume of atmospheric dust through time, and significantly so following the Kasimovian (Late Pennsylvanian). In other words, dust generation and sourcing increased substantially from the pre-Kasimovian to the post-Kasimovian world.

Dust deposits of central equatorial Pangaea (North–Central Appalachian Basin)

The shift to an increasingly dusty atmosphere is qualitatively reflected in the compilation of loess deposits (Figs 2 & 3), but perhaps quantitatively verified by compilations of the ash contents of coals, which are now argued to be a good proxy for atmospheric dust deposition (Large and Marshall 2015; Marshall *et al.* 2016; Large *et al.* 2021). Cecil *et al.* (1985) reported that mean ash content in Lower Pennsylvanian coals of the Northern/Central Appalachian Basin was *c.* 6–8%. However, in the Middle and Upper Pennsylvanian, there were three excursions toward much higher ash contents, culminating in coals of the Dunkard Formation in the latest portion of the Upper Pennsylvanian, reaching a mean ash content of 23%.

Naively, such a long-term increase in ash content would imply an increase in dust deposition rates of 3–4×. However, simple translation from ash contents to dust deposition rates would ignore confounding factors such as ash enrichment by volatile loss during coalification (Large and Marshall 2015; Marshall *et al.* 2016; Large *et al.* 2021), input of mineral matter from surface runoff and groundwater

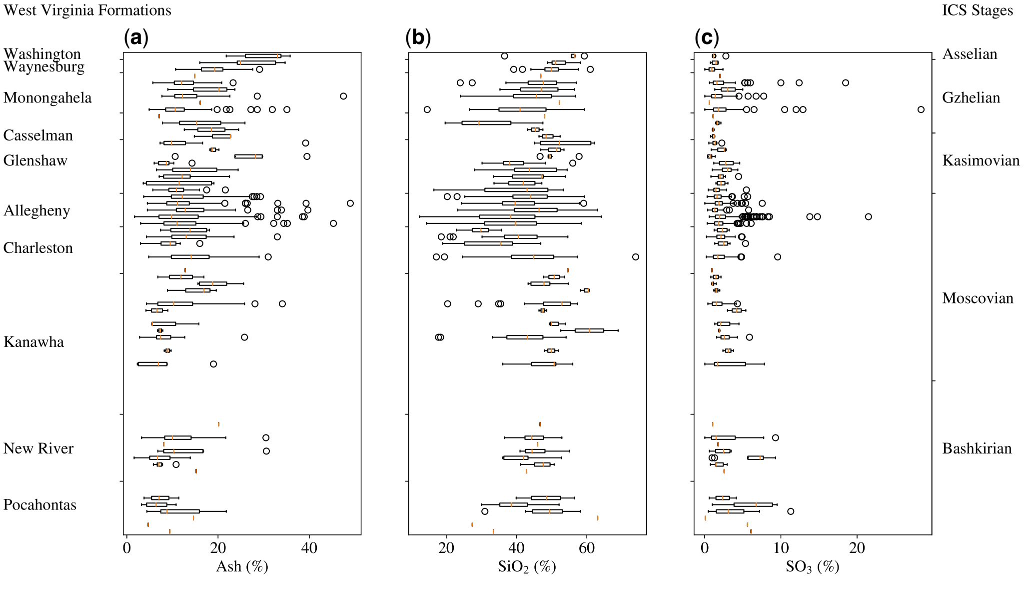

Fig. 5. Box and whisker plot of ash content (%), SiO_2 content (%), and SO_3 content (%) in the sampled coal beds. Orange markers indicate median values (or the only value if there is one sample from the bed). Bed names are omitted for clarity.

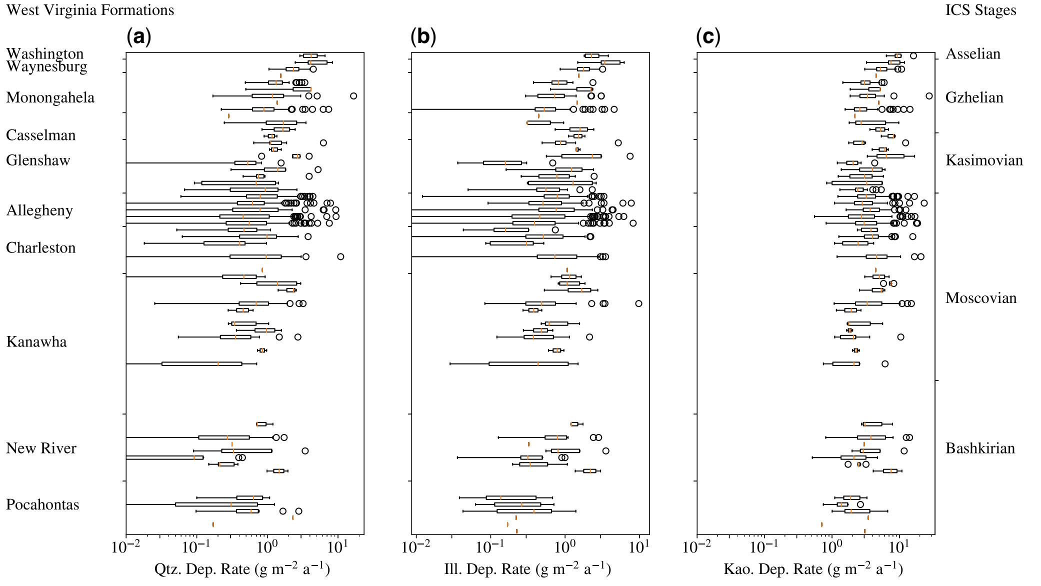

Fig. 6. Box and whisker plot of estimated deposition rates (g m^{-2} a^{-1}) of quartz, illite, and kaolinite. Orange markers indicate median values (or the only value if there is one sample from the bed). Bed names are omitted for clarity.

infiltration rather than airfall deposition (e.g. Shotyk 1988), and input of volcanic ash rather than aeolian dust (e.g. Holmes *et al.* 1999; Chesworth *et al.* 2006; Spears 2012).

As described in Appendix A, we have repeated the analysis of Cecil *et al.* (1985) with an expanded coal chemistry database (Palmer *et al.* 2015) and a method that isolates the deposition of non-volcanic mineral matter that is likely deposited by airfall, enabling a reconstruction of dust deposition in a key region of Central Equatorial Pangaea across the Pennsylvanian.

Ash content variability in the amplified dataset validates the basic pattern found by Cecil *et al.* (1985) (Fig. 5a). Ash is typically low (median value of *c.* 10%) throughout Bashkirian and much of Moscovian time. Later in Moscovian time, extreme values of ash of up to 40% appear, though median ash values remain typical of the earlier period. Median ash values then briefly increase in Kasimovian time, followed by a period of large, extreme values in Gzhelian time, and then an increase to median ash contents of up to 35% in the youngest sampled coals near the Carboniferous–Permian boundary. Thus, ash content throughout coal beds increases about a factor of 3–4 through the Late Carboniferous (Slansky 1984) with some extreme events occurring, particularly later in the Moscovian and in the Gzhelian, which explain the shifts in mean ash content observed by Cecil *et al.* (1985).

There is no particularly strong trend in SiO_2 content (Fig. 5b). Moscovian and Kasimovian coal ashes seem to be slightly less rich in SiO_2 than in other intervals. Median SO_3 values are typically $<5\%$, except in some Bashkirian beds (Fig. 5c). However, extreme values of $>20\%$ occur in some Gzhelian beds and in one bed of Moscovian age, the Middle Kittanning. The significance of SO_3 in coal is disputed. Under most circumstances, S content in coals is proportional to intrusion of marine waters (Chou 2012), so the outlier values may indicate intervals of large sea-level fluctuations.

The reconstructed deposition rates provide a new perspective on the trends in ash content. Kaolinite deposition fluxes are generally dominant (Fig. 6c). Median fluxes vary between 1 and 10 g m^{-2} a^{-1} but typically are fairly close to 3 g m^{-2} a^{-1}. Outlier values of >10 g m^{-2} a^{-1} occur during the Moscovian and Gzhelian. However, there is a definite temporal trend in quartz and illite deposition rates (Fig. 6a, b), with median mineral matter deposition in beds trending richer in quartz and illite toward the Gzhelian and the Asselian. As in the case of kaolinite, outlier values of illite and quartz deposition fluxes are common later in Kasimovian and Gzhelian time. The dominance of kaolinite suggests that these coals largely formed from minerotrophic peats, or else received relatively weathered material from airfall deposition.

Some of this mineral matter was of volcanic origin. Coal ash is moderately enriched in yttrium throughout the Bashkirian and Moscovian, followed by a gradual decrease during the Kasimovian and Gzhelian to the beginning of the Permian (Fig. 7c).

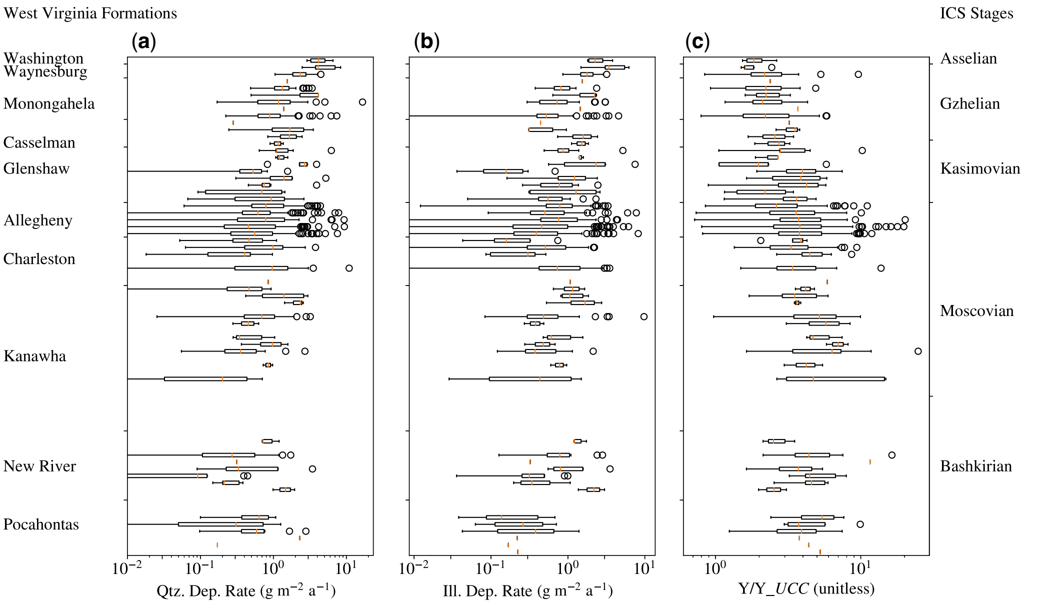

Fig. 7. Box and whisker plot of estimated deposition rates (g m^{-2} a^{-1}) of quartz and illite and of the ratio of Y in ash to Y in UCC (21 ppm). Orange markers indicate median values (or the only value if there is one sample from the bed). Bed names are omitted for clarity.

Outlier values of yttrium enrichment occur later in the Moscovian, suggesting there were occasional, significant contributions from volcanic ashes. Note, however, that the high variability in quartz, illite, and kaolinite deposition later in Moscovian time aligns with high variability in yttrium enrichment.

Corrected for this yttrium enrichment, the pattern of atmospheric dust deposition emerges (Fig. 8a). This dust can be presumed to be distal enough from dust sources to be transported from sufficiently long distances to be <10 µm. Median dust deposition was generally <1 g m^{-2} a^{-1} throughout most of the Late Carboniferous. It increased to *c.* 3 g m^{-2} a^{-1} in particular beds during the Bashkirian and the Kasimovian and reached as high as 7 g m^{-2} a^{-1} late in the Gzhelian. Variability was highest late in Moscovian time, when median dust deposition was *c.* 1 g m^{-2} a^{-1} but possibly up to 10–20 g m^{-2} a^{-1} in individual samples.

The typical level of dust deposition reconstructed during the Late Carboniferous (<1 g m^{-2} a^{-1}) is close to that estimated for Holocene equatorial South America (Albani *et al.* 2015). This level of dust deposition suggests that subtropical dust sources in Pangaea were relatively weak by analogy with present-day South America, where dust deposited in the Amazonian basin is about as influenced by long distance transport from stronger, distal African sources as proximal, weaker sources like the Argentine pampas (Nogueira *et al.* 2021). Dust deposition rates of 3 g m^{-2} a^{-1} would be closer to those modelled in Holocene equatorial Africa, indicating stronger, proximal dust sources (Albani *et al.* 2015). Some upward adjustment must be made to expected dust deposition earlier in the Pennsylvanian, when the area was at higher latitude (van Hinsbergen *et al.* 2015) and closer to speculative dust sources in Gondwanaland inferred from high ash contents in Permian coals from Brazil (Marshall *et al.* 2016). However, this adjustment for latitude is not likely to apply as much for the Moscovian and Gzhelian outlier dust deposition and the peak in median dust deposition late in Gzhelian time. These values are close to *c.* 5–20 g m^{-2} a^{-1} expected for equatorial Africa (up to 10° N) at the Last Glacial Maximum (LGM), which implies dust sources may have been supplied by silt generated by glacial grinding, which must be invoked in climate models to explain increased dust emission and deposition reconstructed for the LGM (Mahowald *et al.* 2006).

The key interpretive factor to keep in mind when thinking about the median, range of variability, and outlier values for a given coal bed is that peat formation in the Appalachian Basin was cyclical; coals appear within fluvial successions interrupted by occasional marine intrusions (e.g. Veevers and Powell 1987; Heckel 1990; Fielding 2021). Forests are more likely to flourish in humid phases, while glacioeustatic sea-level rise and fall can make the difference between peat mires drying out and being

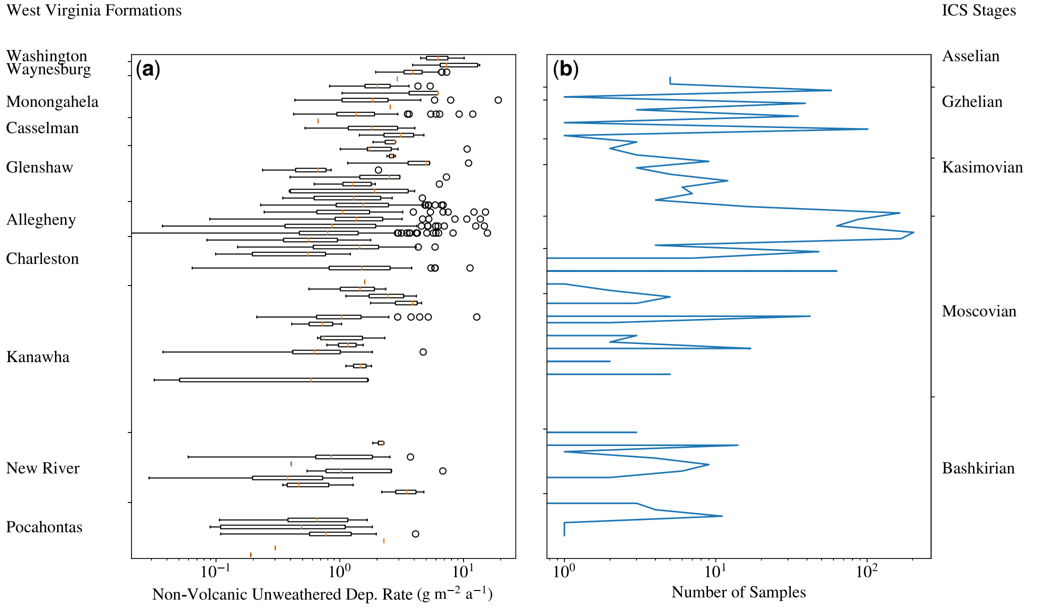

Fig. 8. (**a**) Box and whisker plot of estimated deposition rates (g m^{-2} a^{-1}) of poorly chemical weathered mineral matter from non-volcanic sources. Orange markers indicate median values (or the only value if there is one sample from the bed). (**b**) Number of valid samples used in bed averaging. Bed names are omitted for clarity.

drowned. The hypothesis that coal bed thickness translates into a well-constrained depositional timescale (Large and Marshall 2015; Large *et al.* 2021) suggests that thicker coal beds of a similar grade, age, and palaeolatitude were deposited over a longer time interval than thinner coal beds. These conditions are ably met for the Appalachian Basin coals sampled here.

However, bed or seam thickness (strictly speaking) is not easy to consistently evaluate (Hohn and Britton 2013), and there is no consistently calculated database of seam thickness across the West Virginia coal sequences. The limited data available from Eble *et al.* (2013) suggest that Monongahela Formation (~Gzhelian) coal beds average >4 times the thickness of Washington and Waynesburg Formation (latest Gzhelian–Asselian) coal beds. Thus, coal beds from near the Gzhelian–Asselian boundary are probably sampling the most optimal and presumably most humid period, whereas Gzhelian coals are sampling over a broader climatic range.

In the absence of thickness data, we can use sample number (Fig. 8b) as an approximate proxy. This proxy is not perfect. The Pittsburgh coal bed of the Monongahela Formation (Gzhelian) is the thickest coal bed in the Appalachian Basin (Tewalt *et al.* 2000). However, this analysis suggests that Allegheny Formation (Moscovian) coals are the most thoroughly sampled, even if they are not necessarily as thick as the coals of the Monongahela Formation, and thus they best sample the full spectrum of variability within a glacial–interglacial climate cycle. If this reasoning is valid, then the coals deposited in late Moscovian time and in some parts of Gzhelian time may be capturing drier intervals that are likely missing in the thinner coals of the Waynesburg and Washington formations. But accounting for this difference in sampling leads to two exciting conclusions. First, the subtropics near the Appalachian Basin in late Moscovian time and during the deposition of the Monongahela Formation in Gzhelian time must have experienced an extraordinary amplitude of climate variability from humid to at least semi-arid conditions (with potentially enhanced glacial sediment supply). As this late Moscovian interval also seems to have been a time of significant explosive volcanism near the Appalachian Basin *and* a time of major sea-level excursions and associated marine intrusions (based on SO_3 variability), the late Moscovian captures a time of profound environmental disturbance. This conclusion is substantiated by a broad ecological study of Euramerican coal forests by Falcon-Lang and DiMichele (2010), which found a significant change in diversity and coal forest extent throughout Euramerica across the Moscovian–Kasimovian boundary.

The second conclusion is that the thinner beds of the Washington and Waynesburg (latest Gzhelian–Asselian) may be recording the most humid interval of a relatively arid glacial–interglacial cycle. (Note that, because the correlation between humidity/aridity and glacial/interglacial phases during late Paleozoic time remains disputed (see Heavens *et al.* 2015 and references therein), we speak of the humid and arid phases of a glacial–interglacial cycle rather than the glacial or interglacial phases.) Thus, the median deposition rates should be compared to the lower end of dust deposition rates in the thicker coals of the Monongahela or Allegheny formations, suggesting that dust deposition rates may have increased from *c.* 0.2 g m^{-2} a^{-1} to 7 g m^{-2} a^{-1} in equivalent parts of a glacial–interglacial cycle, indicating a significant increase in aridity and/or sediment supply in dust source regions, even at the most humid point of the cycle.

These data also can be used to test when dust deposition occurred within the glacial cycle, given that the sulfur content in these coals is commonly linked to a marine source (e.g. Chou 2012). In individual Allegheny Formation coal samples, dust deposition is anti-correlated with SO_3 content ($r = -0.22$, $n = 679$, $p = 5\times10^{-9}$). This anti-correlation improves for the logarithm of dust deposition and SO_3 on a linear scale or both on logarithmic scales ($r = -0.43$, $n = 679$, $p = 2\times10^{-32}$; $r = -0.46$, $n = 679$, $p = 3\times10^{-37}$), suggesting that high dust deposition rates and marine intrusions were rarely synchronous. Thus, dust deposition mostly took place at times of lower sea level during glacials, supporting the hypothesis of tropical (or at least subtropical) aridity during glacial phases.

Dust deposits of eastern equatorial Pangaea (western Europe)

The Central Pangaean Mountains formed as the northern supercontinent of Laurussia and southern supercontinent of Gondwanaland began colliding, which progressed roughly from eastern equatorial Pangaea (western Europe) to western equatorial Pangaea (western USA). Hence, the Hercynian–Variscan orogenic belts of western Europe slightly predate those (Appalachian–Ouachita–Marathon) of the USA. The Variscan–Hercynian highlands developed in a long-lived polyphase arc–continent collision (Matte 1986). Many of the upper Paleozoic units appearing in Figure 3 lie preserved in continental basins throughout central and western Europe (Fig. 1; palaeogeographical coordinates) that formed as a result of late Carboniferous syn-orogenic collapse of the overthickened Variscan crust (e.g. Ménard and Molnar 1988; Burg *et al.* 1994; Faure *et al.* 2009). The nature of this syn-orogenic extension ultimately created a dismembered terrane with many discrete intramontane basins that archive correlative records of upper Paleozoic sedimentation derived from erosion of the Variscan Mountains (e.g. Van Den Driessche and Brun 1989; Malavieille *et al.* 1990; Burg *et al.* 1994; Schneider and Scholze 2018). Correlations (cf. Fig. 3; Schneider *et al.* 2006, 2019; Schneider and Lucas 2015) among continental basins within the European Variscan belt continue to improve with emerging radiometric and biostratigraphic data and – where the upper Paleozoic record is complete – stratigraphy includes a 'grey to red' transition near the Asselian–Sakmarian boundary (e.g. Pochat and Van Den Driessche 2011) that is broadly interpreted through continental basins of Laurussia and Gondwana to reflect a shift from wet to dry climates (e.g. Parrish 1993; Schneider *et al.* 2006; Mujal *et al.* 2018), although distinguishing climatic controls from the local and regional extensional tectonic controls in the Variscan belt remains challenging (Pochat and Van Den Driessche 2011). Upper Carboniferous–lower Permian (Gzhelian–Asselian) fluvial–alluvial and lacustrine organic-rich deposits tend to be coal-rich (cf. Autun Basin, France; Mercuzot *et al.* 2022) and locally contain (hypothesized) evidence for periglacial features (cf. Lodève Basin, France; Becq-Giraudon *et al.* 1996; Pfeifer *et al.* 2021*b*). Pervasive redbed deposits that first appear at the Asselian–Sakmarian boundary reflect predominantly 'wet' (fluvial–alluvial) sedimentation in the Sakmarian and Artinskian (e.g. the Rabejac Formation, Lodeve Basin; Lower Nahe Subgroup, Saar–Nahe Basin; Schneider *et al.* 2006 and refs within), but by around the Kungurian (and through the Capitanian) evidence of fluvial systems subsides, replaced by a shift to what have been widely interpreted as playa lake, arid-fan, or floodplain deposits, consisting of large volumes of red mudstone. The lower–middle Salagou Formation in the Lodève Basin (southern France) is among the thickest (>1 km) and most complete record of this fine, almost exclusively red Permian mudstone, but for example (Fig. 3): the Upper Nahe Subgroup (Saar–Nahe Basin), the Eisenach Formation (Thuringian Forest Basin), Trutnov Formation (Krkonose Piedmont and Intrasudetic basins; Schneider *et al.* 2006 and refs within), and Upper Red Unit (Pyrenean Basin; Mujal *et al.* 2018) display analogous silty continental facies and characteristics consistent with oxidation and aridity.

Palaeo-loess units of western equatorial Pangaea were previously interpreted as tidal flat or deltaic shales, yet lack the typical facies attributes of these systems as well as the fluvial feeder systems necessary to deliver such large volumes of fine-grained sediment to the depositional area (e.g. Sweet *et al.* 2013; Foster *et al.* 2014). Using analogous criteria, Pfeifer *et al.* (2021*a*) hypothesized that thick successions of exclusively fine red mudstone in the lower–middle Permian Salagou Formation (Lodève Basin, France) record loess deposition, sourced by the

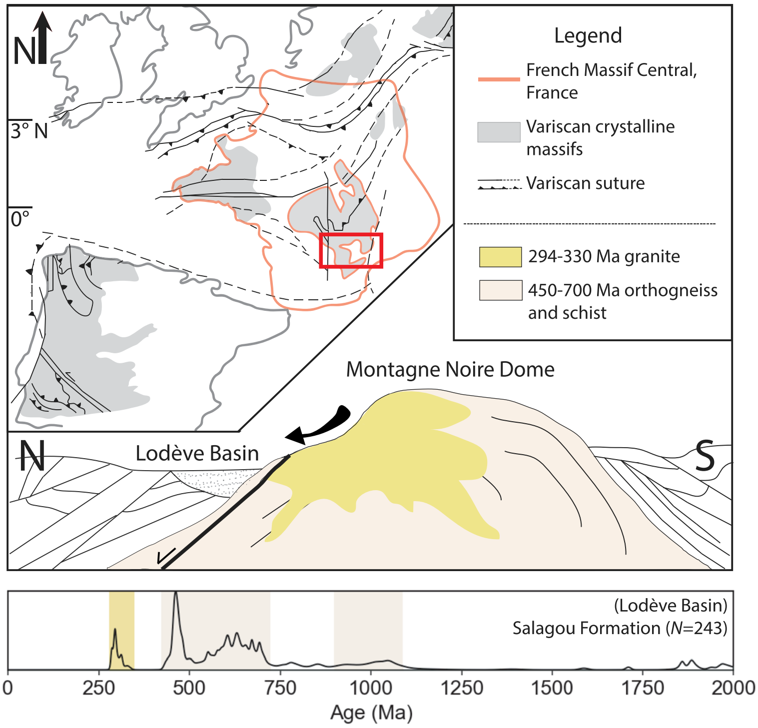

Fig. 9. Provenance of the lower–middle Permian Salagou Formation (Lodève Basin, France). Detrital zircon age spectra from Salagou Formation samples yield three prominent age populations that correspond with the primary lithologies (*c.* 294–330 Ma granites and ≥450 Ma orthogneiss and schist) that comprise the Montagne Noire Dome, a metamorphic core complex that is the interpreted source of Salagou Formation sediment. Inset: Red box denotes the location of the Lodève Basin, southern French Massif Central, France. The French Massif Central is one of many crystalline massifs within the Variscan Mountains of eastern equatorial Pangaea (western Europe). Source: modified from Pfeifer *et al.* (2018).

erosion of local, rapidly-exhuming Variscan palaeohighlands (Fig. 9; Pfeifer *et al.* 2018). And while the Salagou Formation may represent the most complete, and perhaps oldest deposit of Permian loess in western Europe, we speculate that the similar facies attributes of many of the uniformly fine-grained 'playa' and 'floodplain' deposits across western Europe might include unrecognized palaeoloess deposits (e.g. correlative units in other basins in France, Germany, Morocco, Spain mentioned above; Fig. 3). Further investigation is required to test this working hypothesis, and to document the nature and extent of Permian dust deposits in western Europe (in progress; Pfeifer *et al.* 2022), including whether other Permian European loess deposits are also sourced from proximal Variscan palaeo-uplifts. The generation and accumulation of kilometres-thick – and potentially widespread – Permian loess deposits in western Europe has significant palaeoclimatic implications for eastern equatorial Pangaea, and calls into question the conditions that created such large volumes of silt. If this material indeed records dust and loess deposition, it implies widespread dust generation that increased substantially following the Kasimovian, and likely before the Kasimovian.

Discussion: the late Paleozoic dust bowl of equatorial Pangaea

Dust as an archive of climate and climate change in the late Paleozoic

As the most abundant sedimentary deposit on land today (Catt 1988; Li *et al.* 2020), loess is so well known that many have termed it characteristic of the Quaternary (Catt 1988; Smalley 1995; Muhs and Bettis 2003; Li *et al.* 2020). Indeed, Muhs and Bettis (2003) labelled Quaternary loess a 'sedimentary extreme'. There has long been a close genetic association between glaciation and loess, owing to the proximity of the world's large loess deposits to formerly glaciated regions (e.g. many loess deposits of North America and Europe), or catchments downwind of glaciated regions (e.g. the Chinese Loess Plateau), and the known capacity for glaciers to produce silt. But loess also occurs in warm deserts, although the comparably thin and patchy character fuels the persistent controversy regarding the modes of silt generation in these systems: It seems difficult to generate voluminous silt to form loess via aridity alone.

The near ubiquity of loess in the late Cenozoic contrasts with its dearth in most of Earth's Phanerozoic record, outside of the Late Devonian–Permian. Assuming this contrast captures a real phenomenon rather than a simple lack of recognition of deep-time loess, it behooves us to understand the potential implications, and the similarities and differences between Cenozoic and Paleozoic loess.

A major contrast between loess of the Cenozoic and Paleozoic is thickness of the deposits. Inferred palaeo-loess of the late Paleozoic can be an order of magnitude thicker (>>1000 m) than the thickest loess successions of the late Cenozoic (generally *c.* 100 m), although the difference could reflect the persistence of loess-forming conditions over a more prolonged time. Sedimentation rates (neglecting the effects of compaction) of the Maroon Formation palaeo-loess of western equatorial Pangaea (*c.* 70 mm a^{-1}; Soreghan *et al.* 2015) approximate those of the Quaternary Chinese loess (Vandenberghe *et al.* 1997), yet loess deposition in this general region of equatorial Pangaea persisted for as much as 28 myr (approx. middle Late Carboniferous through early Permian).

A second major contrast is the deposition of loess on or near the Equator during the Carboniferous–Permian. Today, significant loess deposits are confined to the mid- or high latitudes (e.g. Catt 1988; Muhs and Bettis 2003; Muhs *et al.* 2014; Li *et al.* 2020). The few exceptions that occur in low-latitude regions (e.g. Nigeria, McTainsh 1987) are so thin that they could not produce anything near the level of thickness of upper Paleozoic loess, even over the space of 28 myr. Explaining the prevalence of loess in late Paleozoic equatorial regions is challenging. Beyond the need for a suitable trapping area, the formation of loess deposits implies a confluence of conditions prevailing within several hundred kilometres (<5°) of the deposit, namely (1) an abundant silt supply; (2) a semi-arid, poorly vegetated surface; and (3) sufficiently high winds to support saltation and dust emission. All these conditions are unusual near the Equator today.

But it is possible to explain the emergence of all these factors in the course of the tectonic and climatic evolution of Pangaea during late Paleozoic time. Silt production is a critical first step. Glacial grinding is a viable way to produce large volumes of silt formed predominantly of primary silicates – that is, clay-poor – (references above). This is the attraction of considering the possibility of glacial silt production in the widespread uplands of the CPMs and associated orogenic systems. This is an admittedly speculative suggestion. Nevertheless, of the few pre-Quaternary loess deposits inferred from non-icehouse intervals (Triassic, Cretaceous), all are rich in clay minerals and/or carbonates (Chan 1999; Jefferson *et al.* 2002; Wilkins *et al.* 2018; Wilson *et al.* 2019; Mao *et al.* 2021), and thus contrast significantly with those of icehouse intervals.

However, non-glacigenic loess is documented in both icehouse and pre-icehouse strata of the Cenozoic: the thickest loess of the Late Pleistocene in North America is the Peoria Loess of the central Great Plains, which exceeds the volume of the glacigenic Peoria Loess along the Mississippi River, and was derived from silt-and very fine sand-rich sources of the (primarily) Oligocene White River and Arikaree groups (Aleinikoff *et al.* 2008). Notably, these sources are predominantly volcanigenic, even interpreted previously as volcaniclastic loess (Hunt 1990; LaGarry 1998). Furthermore, Fan *et al.* (2020) documented significant loess in the late Eocene–Oligocene also sourced in part from volcaniclastic material, but linked to aridification exacerbated by both tectonic uplift and global cooling. A major difference between these examples and those of the late Paleozoic is the lack of a (predominant) volcaniclastic source for the Paleozoic material, especially for western equatorial Pangaea.

Glaciation could form part of the explanation for the widespread appearance of aeolian-marine dusts in the latest Devonian record of western Pangaea (McGlannan *et al.* 2022), which was situated in mid-latitudes at the time, and hosted glaciation in the Appalachian Mountains (Brezinski *et al.* 2008, 2009, 2010). Furthermore, various indicators suggest aridity in the Late Devonian sub-tropics (e.g. Boucot *et al.* 2013), which would have been exacerbated by glaciation. In contrast, eastern equatorial Pangaea was situated nearer the equator during the Late Devonian, with insignificant highlands, and no records of glaciation, nor dust deposits.

As the North American part of Laurussia shifted equatorward (Fig. 1) over Carboniferous time, and with it the Ancestral Rocky Mountains/Midcontinent/Appalachian–Ouachita regions, some silt from Devonian time would remain in the system and gradually be incorporated into long-term sinks. Initially, precipitation was driven by easterly winds emanating from the Palaeo-Tethys, so western equatorial Pangaea would have been slightly drier than eastern equatorial Pangaea (Parrish 1993). Vegetation, including macrofloras, would have spread widely across equatorial Pangaea. Ongoing orogenesis in the Appalachian–Ouachita and Ancestral Rocky

Mountains systems, however, would have altered the precipitation dynamics by creating a double rain shadow between the Ancestral Rocky Mountains and the Ouachitas, gradually aridifying the Midcontinent (recorded by a widespread transition to redbed deposition in the stratigraphic record; cf. Fig. 2).

Simultaneously, mantle flow models show that, in the Late Carboniferous, central-western North America underwent dynamic subsidence (Cocks and Torsvik 2011; Cao *et al.* 2019), resulting in the vast low-lying area of the Midcontinent hosting an epeiric sea, especially at interglacial highstands (e.g. Algeo and Heckel 2008). This seaway helps to explain the very well-known contrast in the S content between coals of the Illinois Basin v. those of the Appalachian Basin; additionally, this sea aided dust trapping. The Midcontinent would have been sensitive to sea-level changes, and the epeiric sea provided a source of additional moisture to support precipitation from airmass thunderstorms, as suggested by climate model simulations (Heavens *et al.* 2015), and the glacial–interglacial variability in macrofloras from dryland to wetland assemblages observed in Atlantic Canada and potentially elsewhere (Falcon-Lang and DiMichele 2010; Falcon-Lang *et al.* 2011). As the Appalachian orogen progressed, crustal loading would have induced further subsidence, magnifying the effects of glacioeustatic changes. In contrast, western-central Europe was the site of (generally) dynamic uplift (cf., Cao *et al.* 2019) associated with construction of the Variscan–Hercynian system – the complement to the Appalachian system of eastern North America.

A vast contraction of swamp forests toward more drought-tolerant species occurred around the time of the Kasimovian (e.g. Phillips *et al.* 1985; DiMichele and Phillips 1996; Cleal and Thomas 2005), recording a significant shift in the equatorial climate system. This shift is attributed to glacial expansion in Gondwanaland, resulting in extreme lowstands and more seasonal precipitation, particularly in western equatorial Pangaea, followed by warming (e.g. Falcon-Lang and DiMichele 2010; Falcon-Lang *et al.* 2011). Using modelling, Richey *et al.* (2020) recently ascribed these vegetational changes to threshold shifts in $p\mathrm{CO_2}$ and precipitation. This shift coincides with the proliferation of palaeo-loess deposits, (e.g. Kessler *et al.* 2001; Soreghan *et al.* 2008) as well as arid-type palaeosols (e.g. Tabor and Montanez 2004).

Thus, western and sometimes central equatorial Pangaea became drier and less vegetated. Furthermore, the windward sides of the Ancestral Rocky Mountains and the Appalachians (i.e. the east and SE) remained quite wet (Peyser and Poulsen 2008; Heavens *et al.* 2015). Under Pleistocene glacial conditions, equilibrium line altitudes for mountain glaciers could reach as low as 3525 m in high precipitation areas near the Equator (Hastenrath 2009), and unstable glacier fronts reached below 2100–2400 m (Osmaston 1989; Kaser and Osmaston 2002), reinforcing the viability of the hypothesis that glacial grinding was possible at elevations above *c.* 2000 m over the largest set of equatorial orogenic belts in the Earth's known history. Admittedly, such a large orogenic system could have exacerbated silt production via processes such as tectonic stresses, in addition to, for example, frost shattering – mechanisms linked to the 'mountain' loess mode (cf. Smalley and Derbyshire 1990; Li *et al.* 2020; Fenn *et al.* 2022), albeit the efficacy of these relative to glacial grinding remains unknown.

Glaciation of the mountain belts would have driven large temperature contrasts across complex topography, likely leading to the development of mesoscale wind systems such as foehn. The initiation of the Pangaean megamonsoon (Soreghan *et al.* 2002; Tabor and Montanez 2002) would have resulted in the development of a low-level jet (Heavens *et al.* 2015) that could have been a source of momentum to be mixed down to the surface during any thunderstorms, though Heavens *et al.* (2015) also suggested that convection and convective precipitation would have been suppressed over the mountain belts if they were substantially glaciated. This reduction of precipitation would have raised the elevation band over which glaciation was stable, but the inherent instability of the system might have led to even more glacial erosion. The monsoon also may have enhanced the seasonality of precipitation or evaporation at the palaeo-equator generally by displacing the inter-tropical convergence zone (ITCZ) from the palaeo-equator in winter and summer (e.g. Peyser and Poulsen 2008; Tabor and Poulsen 2008), but the monsoon simply may have widened the ITCZ rather than displaced it (Heavens *et al.* 2015).

Relative to western equatorial Pangaea, onset of aridification was delayed in the European basins of eastern equatorial Pangaea (Parrish 1993; Rees *et al.* 2002; Tabor and Poulsen 2008). These areas occupied the windward (southeastern) side of the Central Pangaean Mountains and thus remained wet, except perhaps under conditions of widespread local mountain glaciation (Soreghan *et al.* 2022). Consider the stratigraphy of the United Kingdom where coals occur interspersed with and capped by redbeds, suggesting coal forest collapse and more arid conditions by about the latest Kasimovian from the youngest Carboniferous strata in the basins of Bristol and Gloucestershire as well as perhaps slightly later in the Warwickshire Group of the Pennine Basin (Waters *et al.* 2009). This timing seems closer to the Appalachian Basin of central equatorial Pangaea than the French basins to the south of the Variscan front (Pfeifer *et al.* 2021*a*). But because of the possibility of the youngest coals being removed by the Variscan unconformity, it would be worth investigating how dust deposition in coals changed in eastern equatorial Pangaea, which would yield tighter constraints on the timing of aridification.

The significant difference in the proximity of dust/loess accumulation sites to their source regions in eastern (Fig. 9; 10^2 km) v. western (Fig. 4; 10^3 km) Pangaea relates to the lateral variation in tectonic and climatic controls (discussed above) across the equatorial Central Pangean Mountains. In eastern equatorial Pangaea, orogenic collapse produced a dismembered landscape that precluded development of continental-scale river systems, resulting in highland-proximal silt deposition. In southern France, the Salagou Formation loessite accumulated <50 km from its upland source (Fig. 9; Massif Central, France; Pfeifer *et al.* 2018), despite exhibiting a fine grain size mode (10–17 µm) that would likely be interpreted as distal loess in the western US system. This fine mode may reflect the predominant role of aeolian transport here, given the (inferred) lack of involvement of river transport in the ultimate source-to-sink journey. The Salagou Formation and similar, candidate loess correlatives across eastern equatorial Pangaea (Fig. 3) are confined to small, isolated rift basins adjacent to palaeohighlands. Conversely in the west, numerous detrital zircon studies confirm the existence of transcontinental river systems that would have played a key role in transporting the silt from its mountainous source regions (primarily in the Appalachian system and secondarily the ARM; e.g. Gehrels *et al.* 2011; Leary *et al.* 2017, 2020; Chapman and Laskowski 2019; Thomas *et al.* 2020; Lawton *et al.* 2021; Kushner *et al.* 2022), from which the silt could be deflated from floodplains and ultimately deposited thousands of kilometres from its origin (Fig. 4).

Dust as agent of climate change in the late Paleozoic earth system

Geological archives of the late Paleozoic, reviewed above, demonstrate that atmospheric dust – both mineral aerosols and volcanic ash – played an increasingly large role in the low-latitude climate system across Pangaea, especially in post-Kasimovian time. We hypothesize that dust likely played a key role in explaining the peak of the late Paleozoic ice age, as marked by the most widespread glacial deposits in the Asselian (Montañez and Poulsen 2013; Soreghan *et al.* 2019).

Recent research focused on early Permian (Asselian) climate highlights a perplexing issue: How did Earth scrub CO_2 from its atmosphere *c.* 300 Ma, and what were the biospheric consequences? The general story is familiar: throughout most of the Phanerozoic, pCO_2 fluctuated as volcanic outgassing vied with silicate weathering and organic/inorganic carbon burial (Berner 2004; Feulner 2017). To the first order, the unprecedented proliferation of vascular land plants in the Carboniferous explains the pCO_2 low that drove the late Paleozoic icehouse. But the details defy explanation: pCO_2 reached its nadir *c.* 298 Ma (<200 ppm; Montañez *et al.* 2016; Richey *et al.* 2020), whereas the burial flux of terrestrial organic carbon (coal formation) peaked *c.* 20 myr prior (Nelsen *et al.* 2016) – a significant temporal mismatch. Goddéris *et al.* (2017) highlighted this mismatch to argue for the primacy of silicate weathering during peak Pangaean orogenesis to consume pCO_2 and drive the nadir. But more recently, Chen *et al.* (2018) used $^{87}Sr/^{86}Sr$ data to demonstrate reduced continental weathering coincident with the early Permian pCO_2 low, thus challenging the weathering hypothesis. Given the inadequacies of both terrestrial organic carbon burial and continental weathering as viable explanations, Chen *et al.* (2018) cited Sur *et al.*'s (2015) hypothesis of dust-driven fertilization of marine ecosystems that effectively led to a shift in the locus of organic carbon burial to the marine realm.

Sur *et al.* (2015) demonstrated a remarkable finding: enriched values of highly reactive iron in atmospheric dusts from Upper Pennsylvanian–lower Permian loess and related dust across equatorial Pangaea, with major implication for marine carbon cycling. More recently, Sardar Abadi *et al.* (2020) extended Sur *et al.*'s (2015) findings to mid-latitude regions and used lipid biomarker analyses to document high cyanobacterial activity in shallow marine sediments subjected to dust influx. Furthermore, Soreghan *et al.* (2019) documented an especially pronounced peak of explosive felsic-intermediate volcanism *c.* 298–295 Ma – centred spatially at the equator. We speculate that the coincidence of high atmospheric dust loading with high volcanic output would have caused acidic atmospheric processing of dusts that enhanced nutrient (especially iron) bioavailability, thus fertilizing marine ecosystems – likely leading to widespread eutrophia. Subsequently, as Pangaea aridified and epeiric seas dissipated, the potential to sequester carbon via either the mechanisms of silicate weathering or biological carbon burial greatly diminished, leaving few means to scrub the CO_2 that continued to outgas from volcanism, thus enabling a rapid increase in pCO_2 that ultimately initiated the massive collapse of glaciers nearly everywhere but for remnants in highest-latitude Gondwana (Australia). Essentially, volcanic outgassing outpaced the Earth's capacity to sequester atmospheric CO_2.

The early Permian nadir in atmospheric carbon brought the Earth system to near-snowball conditions (Feulner 2017), before pCO_2 levels increased (Montañez *et al.* 2016; Richey *et al.* 2020), leading to the massive loss of ice across most of formerly glaciated Gondwana. Attendant with the well-established record (references above) of non-volcanic mineral aerosols (loess and associated dust deposits) common in the geological record of this early Permian time is a predominance of algal and microbial activity in many epeiric marine ecosystems. Signs of this activity predominate across both shallow-water shelves (Soreghan and Soreghan 2002; Sardar *et al.* 2019), and basins such as the greater Permian Basin, where silt-rich mudstones of the lower Permian host an estimated *c.* 10^{10} metric tonnes of CO_2; USGS 2016, 2018) – a sign of widespread eutrophic conditions – potentially fertilized by dust.

Conclusions

The Late Carboniferous–Permian archives enormous volumes of dust, preserved in both continental (loess) and marine settings. Such vast deposits of dust and loess are unusual in Earth history, and record remarkable atmospheric dustiness in equatorial Pangaea, in contrast with typical occurrences of loess on the modern–recent Earth. Explaining this proliferation of dust begins with generation of the requisite silt-sized material, which cannot be accomplished by aridity alone. Rather, a hypothesis that reconciles the generation, primary silicate composition, and provenance of this vast volume of silt involves glacial grinding and associated erosion in the Central Pangaean Mountains and auxiliary orogenic belts, followed by transport via both rivers and wind deflation. Although dust deposition began in western equatorial Pangaea as early as the latest Devonian (Fammenian) in marine systems, the earliest palaeo-loess deposits date from the Baskirian. In western equatorial Pangaea, the Kasimovian captures the transition between dust trapped in marine systems and the proliferation of true loess deposits. Dust acts as both an archive of Earth's climate, and an agent of climate change. It likely provides at least part of the answer to explaining the temporal discordance between the pCO_2 nadir (associated with peak glaciation) and peak carbon burial by either terrestrial organic carbon (coal formation), or silicate rock weathering (references above).

Acknowledgements Thank you to editors Spencer Lucas and William DiMichele for their encouragement, and to reviewers, especially Joe Mason and an anonymous reviewer, for constructive critiques of the manuscript. Thanks to our international collaborators S. Pochat, J. Van Den Driessche, J. Fortuny, C. Jaime. We respectfully acknowledge the longstanding significance of the lands studied herein for Indigenous Peoples past, present, and future.

Competing interests The authors declare that they have no known competing financial interests or personal relationships that could have appeared to influence the work reported in this paper..

Author contributions **GSS**: conceptualization (lead), data curation (equal), formal analysis (lead), funding acquisition (equal), investigation (lead), methodology (supporting), project administration (lead), supervision (lead), writing – original draft (lead), writing – review & editing (lead); **NGH**: conceptualization (supporting), data curation (lead), funding acquisition (equal), methodology (lead), writing – original draft (supporting), writing – review & editing (supporting); **LSP**: data curation (supporting), formal analysis (supporting), investigation (supporting), methodology (supporting), writing – original draft (supporting), writing – review & editing (supporting); **MJS**: data curation (equal), formal analysis (equal), funding acquisition (equal), methodology (equal), visualization (equal), writing – review & editing (supporting).

Funding Work summarized in this paper was done with funding from the US National Science Foundation under the following EAR grant numbers: 9805130, 0001052, 0230332, 0418983, 0746042, 1053018, 1338331, 1658614 to GSS and MJS, and 1849754 to NGH. Financial support for publication was provided from the Office of the Vice President for Research and Partnerships and the Office of the Provost, University of Oklahoma.

Data availability All data generated or analysed during this study are included in this published article (and its supplementary information files).

References

Adams, S.M. and Soreghan, G.S. 2020. A test of the efficacy of sand saltation for silt production: implications for the interpretation of loess. *Geology*, **48**, https://doi.org/10.1130/G47282.1

Albani, S., Mahowald, N.M. *et al*. 2014. Improved dust representation in the Community Atmosphere Model. *Journal of Advances in Modeling Earth Systems*, **6**, 541–570, https://doi.org/10.1002/2013MS000279

Albani, S., Mahowald, N.M. *et al*. 2015. Twelve thousand years of dust: the Holocene global dust cycle constrained by natural archives. *Climate of the Past*, **11**, 869–903, https://doi.org/10.5194/cp-11-869-2015

Aleinikoff, J.N., Muhs, D.R., Bettis, E.A., III, Johnson, W.C., Fanning, M. and Benton, R. 2008. Isotopic evidence for the diversity of late Quaternary loess in Nebraska: glaciogenic and nonglaciogenic sources. *Geological Society of America Bulletin*, **120**, 1362, https://doi.org/10.1130/B26222.1

Algeo, T.J. and Heckel, P.H. 2008. The Late Pennsylvanian Midcontinent Sea of North America: a review. *Palaeogeography, Palaeoclimatology, Palaeoecology*, **268**, 205–221, https://doi.org/10.1016/j.palaeo.2008.03.049

Alsalem, O.B., Fan, M., Ghosh, N. and Basu, A.R. 2021. Sandstone petrographic and mudstone REE and Nd-isotopic evidence for Middle Pennsylvanian arrival of Gondwana sediments in the Fort Worth Basin. *Palaeogeography, Palaeoclimatology, Palaeoecology*, **579**, 110590, https://doi.org/10.1016/j.palaeo.2021.110590

Assallay, A.M., Rogers, C.D.F., Smalley, I.J. and Jefferson, I.F. 1998. Silt: 2–62 µm, 9–4ϕ. *Earth-Science Reviews*, **45**, 61–88, https://doi.org/10.1016/S0012-8252(98)00035-X

Atkinson, J.D., Murray, B.J. *et al*. 2013. The importance of feldspar for ice nucleation by mineral dust in mixed-phase clouds. *Nature*, **498**, 355–358, https://doi.org/10.1038/nature12278

Balkanski, Y., Schulz, M., Claquin, T., and Guibert, S. 2007. Reevaluation of mineral aerosol radiative forcings suggests a better agreement with satellite and AER- ONET data. *Atmospheric Chemistry and Physics*, **7**, 81–95, https://doi.org/10.5194/acp-7-81-2007

Basarin, B., Buggle, B. *et al*. 2014. Time-scale and astronomical forcing of Serbian loess-paleosol sequences. *Global and Planetary Change*, **122**, 89–106, https://doi.org/10.1016/j.gloplacha.2014.08.007

Becq-Giraudon, J.-F., Montenat, C. and Van Den Driessche, J. 1996. Hercynian high- altitude phenomena in the French Massif Central: tectonic implications. *Palaeogeography, Palaeoclimatology, Palaeoecology*, **122**, 227–241, https://doi.org/10.1016/0031-0182(95)00081-X

Beget, J.E. and Hawkins, D.B. 1989. Influence of orbital parameters on Pleistocene loess deposition in central Alaska. *Nature*, **337**, 151–153, https://doi.org/10.1038/337151a0

Ben-Israel, M., Enzel, Y., Amit, R. and Erel, Y. 2015. Provenance of the various grain-size fractions in the Negev loess and potential changes in major dust sources to the Eastern Mediterranean. *Quaternary Research*, **83**, 105–115, https://doi.org/10.1016/j.yqres.2014.08.001

Berner, R.A. 2004. *The Phanerozoic Carbon Cycle*. Oxford University Press, New York, 158.

Betzer, P.R., Carder, K.L. *et al*. 1988. Long-range transport of giant mineral aerosol particles. *Nature*, **336**, 568–571, https://doi.org/10.1038/336568a0

Blatt, H. 1967. Original characteristics of clastic quartz grains. *Journal of Sedimentary Petrology*, **37**, 401–424.

Blott, S.J. and Pye, K. 2012. Particle size scales and classification of sediment types based on particle size distributions: review and recommended procedures. *Sedimentology*, **59**, 2071–2096, https://doi.org/10.1111/j.1365-3091.2012.01335.x

Boyd, P.W., Law, C.S. *et al*. and 30 others. 2004. The decline and fate of an iron-induced subarctic phytoplankton bloom. *Nature*, **428**, 549–553, https://doi.org/10.1038/nature02437

Boucot, A.J., Xu, C. and Scotese, C.R. 2013. Phanerozoic paleoclimate: an atlas of lithologic indicators of climate. *SEPM Concepts in Sedimentology and Paleontology*, **11**, 1–484.

Bradák, B., Seto, Y., Chadima, M., Kovács, J., Tanos, P., Ujvári, G. and Hyodo, M. 2020. Magnetic fabric of loess and its significance in Pleistocene environment reconstructions. *Earth-Science Reviews*, **210**, 103385, https://doi.org/10.1016/j.earscirev.2020.103385

Breitkreuz, C., Ehling, B.-C. and Sergeev, S. 2009. Chronological evolution of an intrusive/extrusive system: the Late Paleozoic Halle Volcanic Complex in the northeastern Saale Basin (Germany). *Zeitschrift der Deutschen Gesellschaft für Geowissenschaften*, **160**, 173–190, https://doi.org/10.1127/1860-1804/2009/0160-0173

Bressac, M., Guieu, C., Doxaran, D., Bourrin, F., Desboeufs, K., Leblond, N. and Ridame, C. 2014. Quantification of the lithogenic carbon pump following a simulated dust-deposition event in large mesocosms. *Biogeosciences (online)*, **11**, 1007, https://doi.org/10.5194/bg-11-1007-2014

Brezinski, D.K., Cecil, C.B., Skema, V.W. and Stamm, R. 2008. Late Devonian glacial deposits from the eastern United States signal an end of the mid-Paleozoic warm period. *Palaeogeography, Palaeoclimatology, Palaeoecology*, **268**, 143–151, https://doi.org/10.1016/j.palaeo.2008.03.042

Brezinski, D.K., Cecil, C.B., Skema, V.W. and Kertis, C.A. 2009. Evidence for long-term climate change in Upper Devonian strata of the central Appalachians. *Palaeogeography, Palaeoclimatology, Palaeoecology*, **284**, 315–325, https://doi.org/10.1016/j.palaeo.2009.10.010

Brezinski, D.K., Cecil, C.B. and Skema, V.W. 2010. Late Devonian glacigenic and associated facies from the central Appalachian Basin, eastern United States. *Geological Society of America Bulletin*, **122**, 265–281, https://doi.org/10.1130/B26556.1

Bristow, C.S., Drake, N. and Armitage, S. 2009. Deflation in the dustiest place on Earth: the Bodele Depression, Chad. *Geomorphology*, **105**, 50–58, https://doi.org/10.1016/j.geomorph.2007.12.014

Buchwitz, M., Marchetti, L., Jansen, M., Falk, D., Trostheide, F. and Schneider, J. 2020. Ichnotaxonomy and trackmaker assignment of tetrapod tracks and swimming traces from the Middle Permian Hornburg Formation of Saxony-Anhalt (Germany). *Annales Societatis Geologorum Poloniae*, **90**, https://doi.org/10.14241/asgp.2020.23

Buggle, B., Glaser, B., Hambach, U., Gerasimenko, N. and Markovic, S. 2011. An evaluation of geochemical weathering indices in loess-paleosol studies. *Quaternary International*, **240**, 12–21, https://doi.org/10.1016/j.quaint.2010.07.019

Buggle, B., Hambach, U., Müller, K., Zöller, L., Markovic, S.B. and Glaser, B. 2014. Iron mineralogical proxies and quaternary climate change in SE European loess–paleosol sequences. *Catena*, **117**, 4–22, https://doi.org/10.1016/j.catena.2013.06.012

Bullard, J.E., McTainsh, G.H. and Pudmenzky, C. 2004. Aeolian abrasion and modes of fine particle production from natural red dune sands: an experimental study. *Sedimentology*, **51**, 1103–1125, https://doi.org/10.1111/j.1365-3091.2004.00662.x

Bullard, J.E., McTainsh, G.H. and Pudmenzky, C. 2007. Factors affecting the nature and rate of dust production from natural dune sands. *Sedimentology*, **54**, 169–182, https://doi.org/10.1111/j.1365-3091.2006.00827.x

Burchfiel, B.C. and Royden, L.H. 1991. Antler orogeny: a Mediterranean-type orogeny. *Geology*, **19**, 66–69, https://doi.org/10.1130/0091-7613(1991)019<0066:AOAMTO>2.3.CO;2

Burg, J.P., Van Den Driessche, J. and Brun, J.P. 1994. Syn-to-post-thickening extension in the Variscan belt of Western Europe; modes and structural consequences. *Comptes Rendus de l'Academie des Sciences Paris*, **319**, 1019–1032.

Cao, W., Flament, N., Zahirovic, S., Williams, S. and Müller, R.D. 2019. The interplay of dynamic topography and eustasy on continental flooding in the late Paleozoic. *Tectonophysics*, **761**, 108–121, https://doi.org/10.1016/j.tecto.2019.04.018

Carroll, A.R., Stephens, N.P., Hendrix, M.S. and Glenn, C.R. 1998. Eolian-derived siltstone in the Upper Permian Phosphoria Formation: implications for marine upwelling. *Geology*, **26**, 1023–1026, https://doi.org/10.1130/0091-7613(1998)026<1023:EDSITU>2.3.CO;2

Carvajal, C.P., Soreghan, G.S., Isaacson, P.E., Ma, C., Hamilton, M.A., Hinnov, L.A. and Dulin, S.A. 2018. Atmospheric dust from the Pennsylvanian Copacabana Formation (Bolivia): a high-resolution record of paleoclimate and volcanism from northwestern Gondwana. *Gondwana Research*, **58**, 105–121, https://doi.org/10.1016/j.gr.2018.02.007

Cassinis, G., Perotti, C.R. and Ronchi, A. 2012. Permian continental basins in the Southern Alps (Italy) and peri-Mediterranean correlations. *International Journal of Earth Sciences*, **101**, 129–157, https://doi.org/10.1007/s00531-011-0642-6

Catt, J.A. 1988. Loess – its formation, transport and economic significance. *In*: Lerman, A. and Meybeck, M. (eds) *Physical and Chemical Weathering in Geochemical Cycles*. NATO ASI Series (Series C: Mathematical and Physical Sciences), **251**. Springer, Dordrecht, https://doi.org/10.1007/978-94-009-3071-1_6

Cecil, C.B., Stanton, R.W., Neuzil, S.G., Dulong, F.T., Ruppert, L.F. and Pierce, B.S. 1985. Paleoclimate controls on late Paleozoic sedimentation and peat formation in the central Appalachian basin (USA). *International Journal of Coal Geology*, **5**, 195–230, https://doi.org/10.1016/0166-5162(85)90014-X

Cecil, C.B., Hemingway, B.S. and Dulong, F.T. 2018. The chemistry of eolian quartz dust and the origin of chert. *Journal of Sedimentary Research*, **88**, 743–752, https://doi.org/10.2110/jsr.2018.39

Chan, M.A. 1999. Triassic loessite of north-central Utah: stratigraphy, petrophysical character, and paleoclimate implications. *Journal of Sedimentary Petrology*, **69**, 477–485, https://doi.org/10.2110/jsr.69.477

Chapman, A.D. and Laskowski, A.K. 2019. Detrital zircon U–Pb data reveal a Mississippian sediment dispersal network originating in the Appalachian orogen, traversing North America along its southern shelf, and reaching as far as the southwest United States. *Lithosphere*, **11**, 581–587, https://doi.org/10.1130/L1068.1

Chen, J., Montañez, I.P., Qi, Y., Shen, S. and Wang, X. 2018. Strontium and carbon isotopic evidence for decoupling of pCO2 from continental weathering at the apex of the late Paleozoic glaciation. *Geology*, **46**, 395–398, https://doi.org/10.1130/G40093.1

Chesworth, W., Martínez Cortizas, A. and García-Rodeja, E. 2006. The redox–pH approach to the geochemistry of the Earth's land surface, with application to peatlands. *Developments in Earth Surface Processes*, **9**, 175–195, https://doi.org/10.1016/S0928-2025(06)09008-0

Chiu, C.F. and Ng, C.W.W. 2014. Relationships between chemical weathering indices and physical and mechanical properties of decomposed granite. *Engineering Geology*, **179**, 76–89, https://doi.org/10.1016/j.enggeo.2014.06.021

Chou, C.L. 2012. Sulfur in coals: a review of geochemistry and origins. *International Journal of Coal Geology*, **100**, 1–13, https://doi.org/10.1016/j.coal.2012.05.009

Cleal, C.J. and Thomas, B.A. 2005. Palaeozoic tropical rainforests and their effect on global climates: is the past the key to the present? *Geobiology*, **3**, 13–31, https://doi.org/10.1111/j.1472-4669.2005.00043.x

Cocks, L.R.M. and Torsvik, T.H. 2011. The Palaeozoic geography of Laurentia and western Laurussia: a stable craton with mobile margins. *Earth-Science Reviews*, **106**, 1–51, https://doi.org/10.1016/j.earscirev.2011.01.007

Coudé-Gassen, G. 1987. Local, proximal and distal Saharan dusts: Characterization and contribution to the sedimentation. *In*: Leinen, M. and Sarnthein, M. (eds) *Paleoclimatological and Paleometeorology: Modern and Past Patterns of Global Atmospheric Transport*. Kluwer Academic, Norwell, MA.

Crouvi, O., Amit, R., Enzel, Y., Porat, N. and Sandler, A. 2008. Sand dunes as a major proximal dust source for late Pleistocene loess in the Negev Desert, Israel. *Quaternary Research*, **70**, 275–282, https://doi.org/10.1016/j.yqres.2008.04.011

Crouvi, O., Amit, R., Enzel, Y. and Gillespie, A.R. 2010. Active sand seas and the formation of desert loess. *Quaternary Science Reviews*, **29**, 2087–2098, https://doi.org/10.1016/j.quascirev.2010.04.026

De Vleeschouwer, F., Pazdur, A. *et al*. 2012. A millennial record of environmental change in peat deposits from the Misten Bog (East Belgium). *Quaternary International*, **268**, 44–57, https://doi.org/10.1016/j.quaint.2011.12.010

DeMott, P.J., Sassen, K. *et al*. 2003. African dust aerosols as atmospheric ice nuclei. *Geophysical Research Letters*, **30**, 1732, https://doi.org/10.1029/2003GL017410

Dendy, S.N., Guenthner, W.R., Grimley, D.A. and Conroy, J.L. 2021. Detrital zircon geochronology and provenance of Pleistocene loess and contributing glacial sources, midcontinental USA. *Quaternary Science Reviews*, **273**, 107201, https://doi.org/10.1016/j.quascirev.2021.107201

Di Biagio, C., Balkanski, Y., Albani, S., Boucher, O. and Formenti, P. 2020. Direct radiative effect by mineral dust aerosols constrained by new microphysical and spectral optical data. *Geophysical Research Letters*, **47**, https://doi.org/10.1029/2019GL086186

DiMichele, W.A. and Phillips, T.L. 1996. Climate change, plant extinctions and vegetational recovery during the Middle-Late Pennsylvanian Transition: the case of tropical peat-forming environments in North America. *Geological Society, London, Special Publications*, **102**, 201–221, https://doi.org/10.1144/GSL.SP.1996.001.01.14

Dietrich, S. and Seelos, K. 2010. The reconstruction of easterly wind directions for the Eifel region (Central

Europe) during the period 40.3–12.9 ka BP. *Climate of the Past*, **6**, 145–154, https://doi.org/10.5194/cp-6-145-2010

Durant, A.J., Harrison, S.P., Matthew Watson, I. and Balkanski, Y. 2009. Sensitivity of direct radiative forcing by mineral dust to particle characteristics. *Progress in Physical Geography*, **33**, 80–102, https://doi.org/10.1177/0309133309105034

Eble, C.F., Grady, W.C. and Blake, B.M. 2013. Dunkard Group coal beds: palynology, coal petrography and geochemistry. *International Journal of Coal Geology*, **119**, 32–40, https://doi.org/10.1016/j.coal.2013.07.023

Enzel, Y., Amit, R., Crouvi, O. and Porat, N. 2010. Abrasion-derived sediments under intensified winds at the latest Pleistocene leading edge of the advancing Sinai–Negev erg. *Quaternary Research*, **74**, 121–131, https://doi.org/10.1016/j.yqres.2010.04.002

Evans, J.E. and Reed, J.M. 2007. Integrated loessite-paleokarst depositional system, early Pennsylvanian Molas Formation, Paradox Basin, southwestern Colorado, USA. *Sedimentary Geology*, **195**, 162–181, https://doi.org/10.1016/j.sedgeo.2006.07.010

Evans, J.E. and Soreghan, M.J. 2015. Long-distance transport and episodic resedimentation of Pennsylvanian dust (eolian silt) in case passages of the Mississippian Leadville Limestone, southwestern Colorado, USA. *Geological Society of America Special Publication*, **516**, 263–283.

Falcon-Lang, H.J. and DiMichele, W.A. 2010. What happened to the coal forests during Pennsylvanian glacial phases? *Palaios*, **25**, 611–617, https://doi.org/10.2110/palo.2009.p09-162r

Falcon-Lang, H.J., Heckel, P.H. *et al*. 2011. No major stratigraphic gap exists near the Middle–Upper Pennsylvanian (Desmoinesian–Missourian) boundary in North America. *Palaios*, **26**, 125–139, https://doi.org/10.2110/palo.2010.p10-049r

Fan, M., Feng, R., Geissman, J.W. and Poulsen, C.J. 2020. Late Paleogene emergence of a North American loess plateau. *Geology*, **48**, 273–277, https://doi.org/10.1130/G47102.1

Faure, M., Lardeaux, J.-M. and Ledru, P. 2009. A review of the pre-Permian geology of the. Variscan French Massif Central. *Comptes Rendus Geoscience*, **341**, 202–213, https://doi.org/10.1016/j.crte.2008.12.001

Fenn, K., Millar, I.L. *et al*. 2022. The provenance of Danubian loess. *Earth-Science Reviews*, **226**, 103920, https://doi.org/10.1016/j.earscirev.2022.103920

Feulner, G. 2017. Formation of most of our coal brought Earth close to global glaciation. *Proceedings of the National Academy of Sciences*, **114**, 337, https://doi.org/10.1073/pnas.1712062114

Fielding, C.R. 2021. Late Palaeozoic cyclothems – a review of their stratigraphy and sedimentology. *Earth Science Reviews*, **217**, 103612, https://doi.org/10.1016/j.earscirev.2021.103612

Fischer, A.G. and Sarnthein, M. 1988. Airborne silts and dune-derived sands in the Permian of the Delaware basin. *Journal of Sedimentary Petrology*, **58**, 637–643.

Forster, T., Evans, M.E. and Heller, F. 1994. The frequency dependence of lowfield susceptibility in loess sediments. *Geophysical Journal International*, **118**, 636–642, https://doi.org/10.1111/j.1365-246X.1994.tb03990.x

Foster, T.M., Soreghan, G.S., Soreghan, M.J., Benison, K.C. and Elmore, R.D. 2014. Climatic and paleogeographic significance of eolian sediment in the Middle Permian Dog Creek Shale (Midcontinent US). *Palaeogeography, Palaeoclimatology, Palaeoecology*, **402**, 12–29, https://doi.org/10.1016/j.palaeo.2014.02.031

Gabbott, S.E., Zalasiewicz, J., Aldridge, R.J. and Theron, J.N. 2010. Eolian input into the Late Ordovician postglacial Soom Shale, South Africa. *Geology*, **38**, 1103–1106, https://doi.org/10.1130/G31426.1

Gehrels, G.E., Blakey, R., Karlstrom, K.E., Timmons, J.M., Dickinson, W.R. and Pecha, M.E. 2011. Detrital zircon U-Pb geochronology of Paleozoic strata in the Grand Canyon, Arizona. *Lithosphere*, **3**, 183–200, https://doi.org/10.1130/L121.1

Geluk, M. 1958. *Stratigraphy and tectonics of Permo-Triassic basins in the Netherlands and surrounding areas*. Thesis, Universiteit Utrecht.

Goddéris, Y., Donnadieu, Y., Carretier, S., Aretz, M., Dera, G., Macouin, M. and Regard, V. 2017. Onset and ending of the late Palaeozoic ice age triggered by tectonically paced rock weathering. *Nature Geoscience*, **10**, 382–386, https://doi.org/10.1038/ngeo2931

Guieu, C., Ridame, C., Pulido-Villena, E., Bressac, M., Desboeufs, K. and Dulac, F. 2014. Dust deposition in an oligotrophic marine environment: impact on the carbon budget. *Biogeosciences Discuss*, **11**, 1707–1738, https://doi.org/10.5194/bgd-11-1707-2014

Hallam, A. 1984. Pre-quaternary sea-level changes. *Annual Reviews Earth Planetary Science*, **12**, 205–243, https://doi.org/10.1146/annurev.ea.12.050184.001225

Haq, B.U. and Schutter, S.R. 2008. A chronology of Paleozoic sea-level changes. *Science (New York, NY)*, **322**, 64–68, https://doi.org/10.1126/science.1161648

Harms, J.C. 1974. Brushy Canyon Formation, Texas: a deep-water density current deposit. *Geological Society of America Bulletin*, **85**, 1763–1784, https://doi.org/10.1130/0016-7606(1974)85<1763:BCFTAD>2.0.CO;2

Hastenrath, W. 2009. Past glaciation in the tropics. *Quaternary Science Reviews*, **28**, 790–798, https://doi.org/10.1016/j.quascirev.2008.12.004

Heavens, N.G., Mahowald, N.M., Soreghan, G.S., Soreghan, M.J. and Shields, C.A. 2015. A model-based evaluation of tropical climate in Pangaea during the late Palaeozoic Icehouse. *Palaeogeography, Palaeoclimatology, Palaeoecology*, **425**, 109–127, https://doi.org/10.1016/j.palaeo.2015.02.024

Heckel, P.H. 1990. Evidence for global (glacial-eustatic) control over upper Carboniferous (Pennsylvanian) cyclothems in midcontinent North America. *Geological Society, London, Special Publications*, **55**, 35–47, https://doi.org/10.1144/GSL.SP.1990.055.01.02

Heslop, D., Langereis, C.G. and Dekkers, M.J. 2000. A new astronomical timescale for the loess deposits of Northern China. *Earth and Planetary Science Letters*, **184**, 125–139, https://doi.org/10.1016/S0012-821X(00)00324-1

van Hinsbergen, D.J.J., de Groot, L.V. *et al*. 2015. A paleolatitude calculator for paleoclimate studies. *PLoS ONE*, **10**, 6, https://doi.org/10.1371/journal.pone.0126946

Hohn, M.E. and Britton, J.Q. 2013. A geostatistical case study in West Virginia: all coals are not the same.

International Journal of Coal Geology, **112**, 125–133, https://doi.org/10.1016/j.coal.2012.12.004

Holmes, J., Hall, V. and Wilson, P. 1999. Volcanoes and peat bogs. *Geology Today*, **15**, 60–63, https://doi.org/10.1046/j.1365-2451.1999.1502005.x

Hull, J.P.D., Jr 1957. Petrogenesis of Permian Delaware Mountain sandstone, Texas and New Mexico. *American Association of Petroleum Geologists, Bulletin*, **41**, 278–307.

Hunt, R.M., Jr 1990. Taphonomy and sedimentology of Arikaree (lower Miocene) fluvial, eolian, and lacustrine environments, Nebraska and Wyoming: a paleobiota entombed in fine-grained volcaniclastic rocks. *Geological Society of America Special Paper*, **244**, 69–111.

Jefferson, I., Rosenbaum, M. and Smalley, I. 2002. Mercia Mudstone as a Triassic aeolian desert sediment. *Mercian Geologist*, **15**, 157–162.

Ji, J., Balsam, W. and Chen, J. 2001. Mineralogic and climatic interpretations of the Luochuan Loess section (China) based on diffuse reflectance spectrophotometry. *Quaternary Research*, **56**, 23–30, https://doi.org/10.1006/qres.2001.2238

Jickells, T., An, Z. *et al*. 2005. Global iron connections between dust, ocean biogeochemistry and climate. *Science (New York, NY)*, **308**, 67–71, https://doi.org/10.1126/science.1105959

Kaser, G. and Osmaston, H.A. 2002. *Tropical Glaciers (with map of Glaciers and Glaciations of the Rwenzori Mountains, Uganda)*. Cambridge University Press, Cambridge.

Kessler, J.L.P., Soreghan, G.S. and Wacker, H.J. 2001. Equatorial aridity in western Pangea: lower Permian loessite and dolomitic paleosols in northeastern New Mexico, USA. *Journal of Sedimentary Research*, **71**, 817–832, https://doi.org/10.1306/2DC4096B-0E47-11D7-8643000102C1865D

Kluth, C.F. and Coney, P.J. 1981. Plate tectonics of the Ancestral Rocky Mountains. *Geology*, **9**, 10–15, https://doi.org/10.1130/0091-7613(1981)9<10:PTOTAR>2.0.CO;2

Kuenen, P.H. 1960. Experimental abrasion 4: eolian action. *Journal of Geology*, **68**, 427–449, https://doi.org/10.1086/626675

Kushner, B.E., Soreghan, G.S. and Soreghan, M.J. 2022. Late Paleozoic cratonal sink: Distally sourced sediment filled the Anadarko Basin (USA) from multiple source regions. *Geosphere*, **18**, 1831–1850, https://doi.org/10.1130/GES02489.1

LaGarry, H.E. 1998. Lithostratigraphic revision and redescription of the Brule Formation (White River Group) of northwestern Nebraska. *Geological Society of America Special Paper*, **325**, 63–91.

Lagnaoui, A., Voigt, S., Saber, H. and Schneider, J.W. 2014. First occurrence of tetrapod footprints from Westphalian strata of the Sidi Kassem Basin, Central Morocco. *Ichnos*, **21**, 223–233, https://doi.org/10.1080/10420940.2014.955096

Large, D.J. and Marshall, C. 2015. Use of carbon accumulation rates to estimate the duration of coal seams and the influence of atmospheric dust deposition on coal composition. *Geological Society, London, Special Publications*, **404**, 303–315, https://doi.org/10.1144/SP404.15

Large, D.J., Marshall, C., Jochmann, M., Jensen, M., Spiro, B.F. and Olaussen, S. 2021. Time, hydrologic landscape and the long-term storage of peatland carbon in sedimentary basins. *Journal of Geophysical Research: Earth Surface*, **126**, e2020JF005762, https://doi.org/10.1029/2020JF005762

Lawton, T.F., Blakey, R.C., Stockli, D.F. and Liu, L. 2021. Late Paleozoic (Late Mississippian–Middle Permian) sediment provenance and dispersal in western equatorial Pangea. *Palaeogeography, Palaeoclimatology, Palaeoecology*, **572**, 110386, https://doi.org/10.1016/j.palaeo.2021.110386

Leary, R.J., Umhoefer, P., Smith, M.E. and Riggs, N. 2017. A three-sided orogen: a new tectonic model for Ancestral Rocky Mountain uplift and basin development. *Geology*, **45**, 735–738, https://doi.org/10.1130/G39041.1

Leary, R.J., Umhoefer, P. *et al*. 2020. Provenance of Pennsylvanian–Permian sedimentary rocks associated with the Ancestral Rocky Mountains orogeny in southwestern Laurentia: implications for continental-scale Laurentian sediment transport systems. *Lithosphere*, **12**, 88–121, https://doi.org/10.1130/L1115.1

Li, Y., Shi, W., Aydin, A., Beroya-Eitner, M.A. and Gao, G. 2020. Loess genesis and worldwide distribution. *Earth-Science Reviews*, **201**, 102947, https://doi.org/10.1016/j.earscirev.2019.102947

Liu, Y., Liu, X. and Sun, Y. 2021. QGrain: An open-source and easy-to-use software for the comprehensive analysis of grain size distributions. *Sedimentary Geology*, **423**, 105980, https://doi.org/10.1016/j.sedgeo.2021.105980

Livingstone, I. and Warren, A. 1996. *Aeolian Geomorphology*. Longman, Harlow.

Mack, G.H., Leeder, M., Perez-Arlucea, M. and Bailey, B.D.J. 2003. Early Permian silt-bed fluvial sedimentation in the Orogrande basin of the Ancestral Rocky Mountains, New Mexico, USA. *Sedimentary Geology*, **160**, 159–178, https://doi.org/10.1016/S0037-0738(02)00375-5

Maher, B.A. 2011. The magnetic properties of quaternary aeolian dusts and sediments, and their palaeoclimatic significance. *Aeolian Research*, **3**, 87–144, https://doi.org/10.1016/j.aeolia.2011.01.005

Maher, B.A. 2016. Palaeoclimatic records of the loess/palaeosol sequences of the Chinese Loess Plateau. *Quaternary Science Reviews*, **154**, 23–84, https://doi.org/10.1016/j.quascirev.2016.08.004

Mahowald, N.M. 2011. Aerosol indirect effect on biogeochemical cycles and climate. *Science (New York, NY)*, **334**, 794–796, https://doi.org/10.1126/science.1207374

Mahowald, N.M. and Kiehl, L. 2003. Mineral aerosol and cloud interactions. *Geophysical Research Letters*, **30**, https://doi.org/10.109/2002GL016762

Mahowald, N.M., Baker, A. *et al*. 2005. The atmospheric global dust cycle and iron inputs to the ocean. *Global Biogeochemical Cycles*, **19**, GB4025, https://doi.org/10.1029/2004GB002402

Mahowald, N.M., Muhs, D.R., Levis, S., Rasch, P.J., Yoshioka, M., Zender, C.S. and Luo, C. 2006. Change in atmospheric mineral aerosols in response to climate: Last glacial period, preindustrial, modern, and doubled carbon dioxide climates. *Journal of Geophysical Research*, **111**, D10202, https://doi.org/10.1029/2005JD006653

Mahowald, N.M., Ward, D.S. *et al*. 2011. Aerosol impacts on climate and biogeochemistry. *Annual Reviews of Environment and Resources*, **36**, 45–74, https://doi.org/10.1146/annurev-environ-042009-094507

Mahowald, N., Albani, S., Kok, J.F., Engelstaeder, S., Scanza, R., Ward, D.S. and Flanner, M.G. 2014. The size distribution of desert dust aerosols and its impact on the Earth system. *Aeolian Research*, **15**, 53–71, https://doi.org/10.1016/j.aeolia.2013.09.002

Malavieille, J., Guihot, P., Costa, S., Lardeaux, J.M. and Gardien, V. 1990. Collapse of the thickened Variscan crust in the French Massif Central: Mont Pilat extensional shear zone and St. Etienne Late Carboniferous Basin. *Tectonophysics*, **177**, 139–149, https://doi.org/10.1016/0040-1951(90)90278-G

Mao, X., Liu, X. and Zhou, X. 2021. Permo-Triassic aeolian red clay of southwestern England and its palaeoenvironmental implications. *Aeolian Research*, **52**, 100726, ISSN 1875-9637, https://doi.org/10.1016/j.aeolia.2021.100726

Marchetti, L., Ronchi, A., Santi, G. and Voigt, S. 2015. The Gerola Valley site (Orobic Basin, Northern Italy): A key for understanding late Early Permian tetrapod ichnofaunas. *Palaeogeography, Palaeoclimatology, Palaeoecology*, **439**, 97–116, https://doi.org/10.1016/j.palaeo.2015.02.032

Marshall, C., Large, D.J. and Heavens, N.G. 2016. Coal derived rates of atmospheric dust deposition during the Permian. *Gondwana Research*, **31**, 20–29, https://doi.org/10.1016/j.gr.2015.10.002

Martin, J., Gordon, R.M. and Fitzwater, S.E. 1991. The case for iron. *Limnology and Oceanography*, **36**, 1793–1802, https://doi.org/10.4319/lo.1991.36.8.1793

Mason, J.A. 2001. Transport direction of Peoria Loess in Nebraska and implications for loess sources on the central Great Plains. *Quaternary Research*, **56**, 79–86, https://doi.org/10.1006/qres.2001.2250

Mason, J.A. and Jacobs, P.M. 1998. Chemical and particle-size evidence for addition of fine dust to soils of the Midwestern United States. *Geology*, **26**, 1135–1138, https://doi.org/10.1130/0091-7613(1998)026<1135:CAPSEF>2.3.CO;2

Mason, J.A., Nater, E.A., Zanner, C.W. and Bell, J.C. 1999. A new model of topographic effects on the distribution of loess. *Geomorphology*, **28**, 223–236, https://doi.org/10.1016/S0169-555X(98)00112-3

Matsu'ura, T., Miyagi, I. and Furusawa, A. 2011. Late Quaternary cryptotephra detection and correlation in loess in northeastern Japan using cummingtonite geochemistry. *Quaternary Research*, **75**, 624–635, https://doi.org/10.1016/j.yqres.2010.12.004

Matte, P. 1986. Tectonics and plate tectonic models for the Variscan belt of Europe. *Tectonophysics*, **126**, 329–374, https://doi.org/10.1016/0040-1951(86)90237-4

Matte, P. 2001. The Variscan collage and orogeny (480–290 Ma) and the tectonic definition of the Armorica microplate: a review. *Terra nova*, **13**, 122–128, https://doi.org/10.1046/j.1365-3121.2001.00327.x

McGlannan, A., Bonar, A. *et al*. 2022. An eolian dust origin for clastic fines of Devono-Mississippian mudrocks of the greater North American midcontinent. *Journal of Sedimentary Research*, **92**, https://doi.org/10.2110/jsr.2022.013

McTainsh, G. 1987. Desert loess in northern Nigeria. *Zeitschrift für Geomorphologie*, **31**, 145–165, https://doi.org/10.1127/zfg/31/1987/145

Ménard, G. and Molnar, P. 1988. Collapse of a Hercynian Tibetan plateau into a late Paleozoic European Basin and Range province. *Nature*, **334**, 235–237, https://doi.org/10.1038/334235a0

Menéndez, I., Díaz-Hernández, J.L., Mangas, J., Alonso, I. and Sánchez-Soto, P.J. 2007. Airborne dust accumulation and soil development in the North-East sector of Gran Canaria (Canary Islands, Spain). *Journal of Arid Environments*, **71**, 57–81, https://doi.org/10.1016/j.jaridenv.2007.03.011

Mercuzot, M., Bourquin, S. *et al*. 2022. Reconsidering Carboniferous–Permian continental paleoenvironments in eastern equatorial Pangea: facies and sequence stratigraphy investigations in the Autun Basin (France). *International Journal of Earth Sciences*, **111**, 1663–1696, https://doi.org/10.1007/s00531-022-02200-6

Montañez, I.P. and Poulsen, C.J. 2013. The Late Paleozoic ice age: an evolving paradigm. *Annual Review of Earth and Planetary Sciences*, **41**, 629–656, https://doi.org/10.1146/annurev.earth.031208.100118

Montañez, I.P., McElwain, J.C. *et al*. 2016. Climate, *p*CO2 and terrestrial carbon cycle linkages during late Palaeozoic glacial–interglacial cycles. *Nature Geoscience*, **9**, 824–828, https://doi.org/10.1038/ngeo2822

Muhs, D.R. 2013. The geologic records of dust in the Quaternary. *Aeolian Research*, **9**, 3–48, https://doi.org/10.1016/j.aeolia.2012.08.001

Muhs, D.R. and Bettis, E.A., III 2003. Quaternary loess-paleosol sequences as examples of climate-driven sedimentary extremes. *In*: Chan, M.A. and Archer, A.W. (eds) *Extreme Depositional Environments: Mega End Members in Geologic Time*. Geological Society of America, Boulder, 53–74. Special Paper 370.

Muhs, D.R., Bush, C.A., Stewart, K.C., Rowland, T.R. and Crittenden, R.D. 1990. Geochemical evidence of Saharan dust parent material for soils developed on Quaternary limestones of Caribbean and western Atlantic islands. *Quaternary Research*, **33**, 157–177, https://doi.org/10.1016/0033-5894(90)90016-E

Muhs, D.R., McGeehin, J.P., Beann, J. and Fisher, E. 2004. Holocene loess deposition and soil formation as competing processes, Matanuska Valley, southern Alaska. *Quaternary Research*, **61**, 265–276, https://doi.org/10.1016/j.yqres.2004.02.003

Muhs, D.R., Cattle, S.R., Crouvi, O., Rousseau, D.-D., Sun, J. and Zarate, M.A. 2014. Chapter 16: loess records. *In*: Knippertz, P. and Stuut, J-BW. (eds) *Mineral Dust: A Key Player in the Earth System*. Springer, 411–441, https://doi.org/10.1007/978-94-017-8978-3

Mujal, E., Fortuny, J., Marmi, J., Dinarès-Turell, J., Bolet, A. and Oms, O. 2018. Aridification across the Carboniferous–Permian transition in central equatorial Pangea: the Catalan Pyrenean succession (NE Iberian Peninsula). *Sedimentary Geology*, **363**, 48–68, https://doi.org/10.1016/j.sedgeo.2017.11.005

Nawrocki, J., Polechoǹska, O., Bogucki, A. and Lanczont, M. 2006. Palaeowind directions recorded in the youngest loess in Poland and western Ukraine as derived from anisotropy of magnetic susceptibility measurements. *Boreas*, **35**, 266–271, https://doi.org/10.1111/j.1502-3885.2006.tb01156.x

Nelsen, M.P., DiMichele, W.A., Peters, S.E. and Boyce, C.K. 2016. Delayed fungal evolution did not cause the Paleozoic peak in coal production. *PNAS*, **113**, 2442–2447, https://doi.org/10.1073/pnas.1517943113

Newell, N.D., Rigby, J.K., Fischer, A.G., Whiteman, A.J., Hickox, J.E. and Bradley, J.S. 1953. *The Permian Reef Complex of the Guadalupe Mountains Region, Texas and New Mexico: A Study in Paleoecology*. W.H. Freeman and Co., San Francisco.

Nogueira, J., Evangelista, H. and Valeriano, C.D.M. 2021. Dust arriving in the Amazon basin over the past 7500 years came from diverse sources. *Communications Earth & Environment*, **2**, 5, https://doi.org/10.1038/s43247-020-00071-w

Obreht, I., Zeeden, C., Hambach, U., Veres, D., Marković, S.B. and Lehmkuhl, F. 2019. A critical reevaluation of palaeoclimate proxy records from loess in the Carpathian Basin. *Earth Science Reviews*, **190**, 498–520, https://doi.org/10.1016/j.earscirev.2019.01.020

Oordt, A.J., Soreghan, G.S., Stemmerik, L. and Hinnov, L.A. 2020. A record of dust deposition in northern, mid-latitude Pangaea during peak icehouse conditions of the late Paleozoic ice age. *Journal of Sedimentary Research*, **90**, 337–363, https://doi.org/10.2110/jsr.2020.15

Opluštil, S., Schmitz, M., Kachlík, V. and Štamberg, S. 2016. Re-assessment of lithostratigraphy, biostratigraphy, and volcanic activity of the Late Paleozoic Intra-Sudetic, Krkonoše-Piedmont and Mnichovo Hradiště basins (Czech Republic) based on new U-Pb CA-ID-TIMS ages. *Bulletin of Geosciences*, **91**, 399–432, https://doi.org/10.3140/bull.geosci.1603

Osmaston, H. 1989. Glaciers, glaciations and equilibrium line altitudes on the Ruwenzori. *In*: Mahaney, W.C. (ed.) *Quaternary and Environmental Research on East African Mountains*. Balkema, Rotterdam, 31–104.

Palmer, C.A., Oman, C.L. and Park, A.J. 2015. The U.S. Geological Survey coal quality (COALQUAL) database version 3.0, USGS Data Series no. 975, https://doi.org/10.3133/ds975

Parrish, J.T. 1993. Climate of the Supercontinent Pangea. *The Journal of Geology*, **101**, 215–233, https://doi.org/10.1086/648217

Peyser, C.E. and Poulsen, C.J. 2008. Controls on Permo-Carboniferous precipitation over tropical Pangaea: a GCM sensitivity study. *Palaeogeography, Palaeoclimatology, Palaeoecology*, **268**, 181–192, https://doi.org/10.1016/j.palaeo.2008.03.048

Pfeifer, L.S., Soreghan, G.S., Pochat, S., Driessche, J.V.D. and Thomson, S.N. 2018. Permian exhumation of the Montagne Noire core complex recorded in the Graissessac-Lodeve Basin, France. *Basin Research*, **30**, 1–14, https://doi.org/10.1111/bre.12197

Pfeifer, L.S., Hinnov, L., Zeeden, C., Rolf, C., Laag, C. and Soreghan, G.S. 2020. Rock magnetic cyclostratigraphy of Permian loess in Eastern Equatorial Pangea (Salagou Formation, south central France). *Frontiers in Earth Science*, **8**, 1–13, https://doi.org/10.3389/feart.2020.00241

Pfeifer, L.S., Soreghan, G.S., Pochat, S. and Van Den Driessche, J. 2021*a*. Loess in eastern equatorial Pangea archives a dusty atmosphere and possible upland glaciation. *GSA Bulletin*, **133**, 379–392, https://doi.org/10.1130/B35590.1

Pfeifer, L.S., Birkett, B.A., Driessche, J., Van Den Driessche Pochat, S. and Soreghan, G.S. 2021*b*. Ice-crystal traces imply ephemeral freezing in early Permian equatorial Pangea. *Geology*, **49**, 1397–1401, https://doi.org/10.1130/G49011.1

Pfeifer, L.S., Soreghan, G.S., Van Den Driessche, J. and Pochat, S. 2022. *Paleo-Loess from the Late Paleozoic of Eastern Equatorial Pangaea [Abstract]*. INQUA LoessFest, China.

Phillips, T.L., Peppers, R.A. and DiMichele, W.A. 1985. Stratigraphic and interregional changes in Pennsylvanian coal swamp vegetation: environmental inferences. *International Journal Coal Geology*, **5**, 43–109, https://doi.org/10.1016/0166-5162(85)90010-2

Pochat, S. and Van Den Driessche, J. 2011. Filling sequence in Late Paleozoic continental basins: A chimera of climate change? A new light shed given by the Graissessac – Lodève basin (SE France). *Palaeogeography, Palaeoclimatology, Palaeoecology*, **302**, 170–186, https://doi.org/10.1016/j.palaeo.2011.01.006

Porter, S.C. 2001. Chinese loess record of monsoon climate during the last glacial–interglacial cycle. *Earth-Science Reviews*, **54**, 115–128, https://doi.org/10.1016/S0012-8252(01)00043-5

Pye, K. 1987. *Aeolian Dust and Dust Deposits*. Academic Press, San Diego, CA.

Pye, K. 1995. The nature, origin, and accumulation of loess. *Quaternary Science Reviews*, **14**, 653–667, https://doi.org/10.1016/0277-3791(95)00047-X

Qi, X. 2016. An icehouse dust record from the Upper Paleozoic (Asselian–Artinskian, Moscovian) Akiyoshi Limestone, Japan. M.S. Thesis, University of Oklahoma, Norman, OK, https://hdl.handle.net/11244/44224

Radczewski, O.E. 1955. Eolian deposits in marine sediments. *SEPM Society for Sedimentary Geology Special Publication*, **4**, https://doi.org/10.2110/pec.55.04

Rea, D.K. 2009. Eolian dust, marine sediments. *In*: Gornitz, V. (ed.) *Encyclopedia of Paleoclimatology and Ancient Environments*. Springer, 308–312, https://doi.org/10.1007/978-1-4020-4411-3

Rea, D.K., Leinen, M. and Janecek, T.R. 1985. Geologic approach to the long-term history of atmospheric circulation. *Science (New York, NY)*, **227**, 1–5.

Rees, P.M., Ziegler, A.M., Gibbs, M.T., Kutzbach, J.E., Behling, P.J. and Rowley, D.B. 2002. Permian phytogeographic patterns and climate data/model comparisons. *Journal of Geology*, **110**, 1–31, https://doi.org/10.1086/324203

Reheis, M.C., Goodmacher, J.C. *et al*. 1995. Quaternary soils and dust deposition in southern Nevada. *Geological Society of America Bulletin*, **107**, 1003–1022, https://doi.org/10.1130/0016-7606(1995)107<1003:QSADDI>2.3.CO;2

Richey, J.D., Montanez, I.P., Godderis, Y., Looy, C.V., Griffis, N.P. and DiMichele, W.A. 2020. Influence of temporally varying weatherability on CO2–climate coupling and ecosystem change in the late Paleozoic. *Climate of the Past*, **16**, 1759–1775, https://doi.org/10.5194/cp-16-1759-2020

Rosenfeld, D., Rudich, Y. and Lahav, R. 2001. Desert dust suppressing precipitation: a possible desertification feedback loop. *Proceedings of the National Academy of Sciences*, **98**, 5975–5980, https://doi.org/10.1073/pnas.101122798

Sardar, M., Soreghan, G.S., Heavens, N.G., Voeten, D.F.A.E. and Ivanova, R.M. 2019. Warm-water carbonates in proximity to Gondwanan ice sheets: a record from the Upper Paleozoic of Iran Paleo-Tethys. *Palaeogeography, Palaeoclimatology, Palaeoecology*, **531**, 108914, https://doi.org/10.1016/j.palaeo.2018.09.008

Sardar Abadi, M., Owens, J.D., Liu, X., Them, T.R., II, Cui, X., Heavens, N.G. and Soreghan, G.S. 2020. Atmospheric dust stimulated marine primary productivity during Earth's penultimate icehouse. *Geology*, **48**, 247–251, https://doi.org/10.1130/G46977.1

Schäfer, A. 2012. Lacustrine environments in Carboniferous–Permian Saar-Nahe Basin, southwest Germany. *American Association of Petroleum Geologists Memoirs*, **95**, https://doi.org/10.1306/13291397M953495

Schneider, J.W. and Scholze, F. 2018. Late Pennsylvanian–Early Triassic conchostracan biostratigraphy: a preliminary approach? *Geological Society, London, Special Publications*, **450**, 365–386, https://doi.org/10.1144/SP450.6

Schneider, J.W. and Lucas, S.G. 2015. Late Carboniferous–Permian-Early Triassic Nonmarine-Marine Correlation: Call for global cooperation. *Permophiles Report on the First International Congress on Continental Ichnology [ICCI-2015]*, El Jadida, Morocco. 21–25.

Schneider, J.W., Körner, F., Roscher, M., and Kroner, U. 2006. Permian climate development in the northern peri-Tethys area – the Lodève basin, French Massif Central, compared in a European and global context. *Palaeogeography, Palaeoclimatology, Palaeoecology*, **240**, 161–183, https://doi.org/10.1016/j.palaeo.2006.03.057

Schneider, J., Rößler, R., Werneburg, R., Scholze, F. and Voigt, S. 2014. Part II. The Carboniferous-Permian basins in Saxony, Thuringia, and Saxony-Anhalt of East Germany. *Wissenschaftliche Mitteilungen, Technische Universität Bergakademie Freiberg, Institut für Geologie*, **46**, 55–121.

Schneider, J.W., Lucas, S.G. *et al*. 2019. Late Paleozoic–early Mesozoic continental biostratigraphy – links to the Standard Global Chronostratigraphic Scale. *Palaeoworld*, **29**, 186–238, https://doi.org/10.1016/j.palwor.2019.09.001

Scotese, C.R. 2021. An atlas of Phanerozoic paleogeographic maps: the seas come in and the seas go out. *Annual Review of Earth and Planetary Sciences*, **49**, 679–728, https://doi.org/10.1146/annurev-earth-081320-064052

Shotyk, W. 1988. Review of the inorganic geochemistry of peat and peatland waters. *Earth Science Reviews*, **25**, 95–176, https://doi.org/10.1016/0012-8252(88)90067-0

Sjöström, J.K., Martínez Cortizas, A. *et al*. 2020. Paleodust deposition and peat accumulation rates–bog size matters. *Chemical Geology*, **554**, 119795, https://doi.org/10.1016/j.chemgeo.2020.119795

Slansky, J.M. 1984. Normative mineral composition of high-temperature coal ashes from the Sydney Basin Coalfields, Australia. *International Journal of Coal Geology*, **4**, 249–262, https://doi.org/10.1016/0166-5162(84)90017-X

Smalley, I.J. 1966. The properties of glacial loess and the formation of loess deposits. *Journal of Sedimentary Research*, **36**, 669–676, https://doi.org/10.1306/74D7153C-2B21-11D7-8648000102C1865D

Smalley, I.J. 1995. Making the material: The formation of silt-sized primary mineral particles for loess deposits. *Quaternary Science Reviews*, **14**, 645–651, https://doi.org/10.1016/0277-3791(95)00046-1

Smalley, I.J. and Derbyshire, E. 1990. The definition of 'ice-sheet' and 'mountain' loess. *Area*, **22**, 300–301.

Smalley, I.J. and Krinsley, D.H. 1978. Loess deposits associated with deserts. *Catena*, **5**, 53–66, https://doi.org/10.1016/S0341-8162(78)80006-X

Smalley, I.J. and Marković, S.B. 2014. Loessification and hydroconsolidation: there is a connection. *Catena*, **117**, 94–99, https://doi.org/10.1016/j.catena.2013.07.006

Smalley, I.J., Jefferson, I.F., Dijkstra, T.A. and Derbyshire, E. 2001. Some major events in the development of the scientific study of loess. *Earth Science Reviews*, **54**, 5–18, https://doi.org/10.1016/S0012-8252(01)00038-1

Smalley, I.J., O'Hara-Dhand, K., Wint, J., Machalett, B., Jary, Z. and Jefferson, I. 2009. Rivers and loess: the significance of long river transportation in the complex event-sequence approach to loess deposit formation. *Quaternary International*, **198**, 7–18, https://doi.org/10.1016/j.quaint.2008.06.009

Smith, G.A. and Lowe, D.R. 1991. Lahars: volcano-hydrologic events and deposition in the debris flow – hyperconcentrated flow continuum. *SEPM Special Publication*, **45**, 59–70.

Soreghan, G.S. 1992. Preservation and paleoclimatic significance of eolian dust in the Ancestral Rocky Mountains province. *Geology*, **20**, 1111–1114, https://doi.org/10.1130/0091-7613(1992)020<1111:PAPSOE>2.3.CO;2

Soreghan, G.S. and Soreghan, M.J. 2002. Atmospheric dust and algal dominance in the late Paleozoic: a hypothesis. *Journal of Sedimentary Research*, **72**, 457–461, https://doi.org/10.1306/011102720457

Soreghan, G.S., Elmore, R.D., Katz, B., Cogoini, M. and Banerjee, S. 1997. Pedogenically enhanced magnetic susceptibility variations preserved in Paleozoic loessite. *Geology*, **25**, 1003–1006, https://doi.org/10.1130/0091-7613(1997)025<1003:PEMSVP>2.3.CO;2

Soreghan, G.S., Soreghan, M.J. and Hamilton, M.A. 2008. Origin and significance of loess in Late Paleozoic western Pangaea: a record of tropical cold? *Palaeogeography, Palaeoclimatology, Palaeoecology*, **268**, 234–259, https://doi.org/10.1016/j.palaeo.2008.03.050

Soreghan, G.S., Heavens, N.G., Hinnov, L.A., Aciego, S.M. and Simpson, C. 2015. Reconstructing the dust cycle in deep time: The case of the Late Paleozoic icehouse. *The Paleontological Society Papers*, **21**, 38, https://doi.org/10.1017/S1089332600002977

Soreghan, G.S., Soreghan, M.J. and Heavens, N.G. 2019. Explosive volcanism as a key driver of the late Paleozoic ice age. *Geology*, **47**, 1–5, https://doi.org/10.1130/G46349.1

Soreghan, G.S., Pfeifer, L.S., Sweet, D.E. and Heavens, N.G. 2022. Detecting upland glaciation in Earth's pre-Pleistocene record. *Frontiers in Earth Science*, **10**, 904787, https://doi.org/10.3389/feart.2022.904787

Soreghan, M.J. and Soreghan, G.S. 2007. Whole-rock geochemistry of Upper Paleozoic loessite, western Pangea: implications for paleo-atmospheric circulation. *Earth and Planetary Science Letters*, **255**, 117–132, https://doi.org/10.1016/j.epsl.2006.12.010

Soreghan, M.J., Soreghan, G.S. and Hamilton, M.A. 2002. Paleowinds inferred from detrital-zircon geochronology of upper Paleozoic loessite, western equatorial Pangea. *Geology*, **30**, 695–698, https://doi.org/10.1130/0091-7613(2002)030<0695:PIFDZG>2.0.CO;2

Soreghan, M.J., Heavens, N., Soreghan, G.S., Link, P.K. and Hamilton, M.A. 2014. Abrupt and high-magnitude changes in atmospheric circulation recorded in the Permian Maroon Formation, tropical Pangaea. *Geological Society of America Bulletin*, **126**, 569–584, https://doi.org/10.1130/B30840.1

Soreghan, M.J., Swift, M. and Soreghan, G.S. 2018. Provenance of Permian eolian and related strata in the North American midcontinent: tectonic and climatic controls on sediment dispersal in western tropical Pangea. *Geological Society of America Special Paper*, **28**, 1–27.

Spears, D.A. 2012. The origin of tonsteins, an overview, and links with seatearths, fireclays, and fragmental rocks. *International Journal of Coal Geology*, **94**, 22–31, https://doi.org/10.1016/j.coal.2011.09.008

Speed, R.C. and Sleep, N.H. 1982. Antler orogeny and foreland basin: a model. *Geological Society of America Bulletin*, **93**, 815–828, https://doi.org/10.1130/0016-7606(1982)93<815:AOAFBA>2.0.CO;2

Sprafke, T., Schulte, P. *et al.* 2020. Paleoenvironments from robust loess stratigraphy using high-resolution color and grain-size data of the last glacial Krems-Wachtberg record (NE Austria). *Quaternary Science Reviews*, **248**, 106602, https://doi.org/10.1016/j.quascirev.2020.106602

Steinmann, P. and Shotyk, W. 1997. Geochemistry, mineralogy, and geochemical mass balance on major elements in two peat bog profiles (Jura Mountains, Switzerland). *Chemical Geology*, **138**, 25–53, https://doi.org/10.1016/S0009-2541(96)00171-4

Stevens, T., Palk, C., Carter, A., Lu, H. and Clift, P.D. 2010. Assessing the provenance of loess and desert sediments in northern China using U–Pb dating and morphology of detrital zircons. *Geological Society of America Bulletin*, **122**, 1331–1344, https://doi.org/10.1130/B30102.1

Stuut, J.-B., Zabel, M., Ratmeyer, V., Helmke, P. and Schefuß, E. 2005. Provenance of present-day eolian dust collected off NW Africa. *Journal of Geophysical Research*, **110**, D04202, https://doi.org/10.1029/2004JD005161

Stuut, J.-B., Smalley, I. and O'Hara-Dhand, K. 2009. Aeolian dust in Europe: African sources and European deposits. *Quaternary International*, **198**, 234–245, https://doi.org/10.1016/j.quaint.2008.10.007

Sur, S., Soreghan, M.J., Soreghan, G.S. and Stagner, A.F. 2010. Extracting the mineral fraction from ancient carbonate: assessing the geologic record of dust. *Journal of Sedimentary Research*, **80**, 763–769, https://doi.org/10.2110/jsr.2010.068

Sur, S., Owens, J.D., Soreghan, G.S., Lyons, T.W., Raiswell, R., Heavens, N.G. and Mahowald, N.M. 2015. Extreme eolian delivery of reactive iron to late Paleozoic icehouse seas. *Geology*, **12**, 1099–1102, https://doi.org/10.1130/G37226.1

Swap, R., Garstang, M., Greco, S., Talbot, R. and Kallberg, P. 1992. Saharan dust in the Amazon Basin. *Tellus*, **44B**, 133–149, https://doi.org/10.3402/tellusb.v44i2.15434

Swart, P.K., Oehlert, A.M., Mackenzie, G.J., Eberli, G.P. and Reijmer, J.J.G. 2014. The fertilization of the Bahamas by Saharan dust: a trigger for carbonate precipitation? *Geology*, **42**, 671–674, https://doi.org/10.1130/G35744.1

Sweet, A.C., Soreghan, L.S., Sweet, D.E., Soreghan, M.J. and Madden, A.S. 2013. Permian dust in Oklahoma: source and origin for middle Permian (Flowerpot-Blaine) redbeds in western tropical Pangaea. *Sedimentary Geology*, **284–285**, 181–196, https://doi.org/10.1016/j.sedgeo.2012.12.006

Swet, N., Elperin, T., Kok, J.F., Martin, R.L., Yizhaq, H. and Katra, I. 2019. Can active sands generate dust particles by wind-induced processes? *Earth and Planetary Science Letters*, **506**, 371–380, https://doi.org/10.1016/j.epsl.2018.11.013

Tabor, N.J. and Montanez, L.P. 2002. Shifts in late Paleozoic atmospheric circulation over western equatorial Pangea: insights from pedogenic mineral ∂18O compositions. *Geology*, **30**, 1127–1130, https://doi.org/10.1130/0091-7613(2002)030<1127:SILPAC>2.0.CO;2

Tabor, N.J. and Montanez, I.P. 2004. Morphology and distribution of fossil soils in the Permo-Pennsylvanian Wichita and Bowie Groups, north-central Texas, USA: implications for western equatorial Pangean palaeoclimate during icehouse–greenhouse transition. *Sedimentology*, **51**, 851–884, https://doi.org/10.1111/j.1365-3091.2004.00655.x

Tabor, N.J. and Poulsen, C.J. 2008. Palaeoclimate across the late Pennsylvanian–early Permian tropical paleolatitudes: a review of climate indicators, their distribution, and relation to palaeophysiographic climate factors. *Palaeogeography, Palaeoclimatology, Palaeoecology*, **268**, 293–310, https://doi.org/10.1016/j.palaeo.2008.03.052

Tarling, D.H. and Hrouda, F. 1993. *The Magnetic Anisotropy of Rocks*. Chapman and Hall, London.

Tegen, I., Lacis, A.A. and Fund, I. 1996. The influence on climate forcing of mineral aerosols from disturbed soils. *Nature*, **380**, 419–422, https://doi.org/10.1038/380419a0

Tewalt, S.J., Ruppert, L.F., Bragg, L.J., Carlton, R.W., Brezinski, D.K., Wallack, R.N. and Butler, D.T. 2000. Chapter C – a digital resource model of the Upper Pennsylvanian Pittsburgh Coal Bed, Monongahela Group, Northern Appalachian Basin Coal Region. *US Geological Survey Professional Paper*, **1625–C**, 106.

Thomas, W.A., Gehrels, G.E. *et al*. 2020. Detrital zircons and sediment dispersal in the eastern Midcontinent of North America. *Geosphere*, **16**, 807–840, https://doi.org/10.1130/GES02152.1

Tobo, Y., Adachi, K., DeMott, P.J., Hill, T.C.J., Hamilton, D.S., Mahowald, N.M. and Nagatsuka, N. 2019. Glacially sourced dust as a potentially significant source of ice nucleating particles. *Nature Geoscience*, **12**, 253–258, https://doi.org/10.1038/s41561-019-0314-x

Torres-Padrón, M.E., Gelado-Caballero, M.D., Collado-Sánchez, C., Siruela-Matos, V.F., Cardona-Castellano, P.J. and Hernández-Brito, J.J. 2002. Variability of dust inputs to the CANIGO zone. *Deep Sea Research Part II: Topical Studies in Oceanography*, **49**, 3455–3464, https://doi.org/10.1016/S0967-0645(02)00091-7

Tsoar, H. and Pye, K. 1987. Dust transport and the question of desert loess formation. *Sedimentology*, **34**, 139–153, https://doi.org/10.1111/j.1365-3091.1987.tb00566.x

Újvári, G., Kok, J.F., Varga, G. and Kovács, J. 2016. The physics of wind-blown loess: implications for grain size proxy interpretations in quaternary paleoclimate studies. *Earth-Science Reviews*, **154**, 247–278, https://doi.org/10.1016/j.earscirev.2016.01.006

USGS 2016. *Assessment of Undiscovered Continuous Oil Resources in the Wolfcamp Shale of the Midland Basin, Permian Basin Province, Texas*. National and Global Petroleum Assessment, https://doi.org/10.3133/fs20163092

USGS 2018. *Assessment of Undiscovered Continuous Oil and Gas Resources in the Wolfcamp Shale and Bone Spring Formation of the Delaware Basin, Permian Basin Province, New Mexico and Texas*. National and Global Petroleum Assessment, https://doi.org/10.3133/fs20183073

Van Den Driessche, J. and Brun, J.P. 1989. Un modèle cinématique de l'extension paleozoique superieur dans le sud du Massif Central. *Comptes Rendus de l'Academie des Sciences Paris*, **309**, 1607–1613.

Vandenberghe, J., Zhisheng, A., Nugteren, G., Huayu, L. and Van Huissteden, K. 1997. New absolute time scale for the Quaternary climate in the Chinese Loess region by grain-size analysis. *Geology*, **25**, 35–38, https://doi.org/10.1130/0091

Van der Does, M., Knippertz, P., Zschenderlein, P., Harrison, P.G. and Stuut, J.-B.W. 2018. The mysterious long-range transport of giant mineral dust particles. *Science Advances*, **4**, 12, https://doi.org/10.1126/sciadv.aau2768

Veevers, J.J. and Powell, C.M. 1987. Late Paleozoic glacial episodes in Gondwanaland reflected in transgressive-regressive depositional sequences in Euramerica. *GSA Bulletin*, **98**, 475–487, https://doi.org/10.1130/0016-7606(1987)98<475:LPGEIG>2.0.CO;2

Vinchon, C. 1984. *Sédimentogenèse et métallogenèse du Permien du dôme du Barrot (Alpes Maritimes, France)*. Documents du BRGM n° 70.

Voigt, S., Hminna, A., Saber, H., Schneider, J.W. and Klein, H. 2010. Tetrapod footprints from the uppermost level of the Permian Ikakern Formation (Argana Basin, Western High Atlas, Morocco). *Journal of African Earth Sciences*, **57**, 470–478, https://doi.org/10.1016/j.jafrearsci.2009.12.003

Washington, R.M., Todd, C., Middleton, N. and Goudie, A.S. 2003. Dust-storm source areas determined by the total ozone monitoring spectrometer and surface observations. *Annals of the American Association of Geographers*, **93**, 297–313, https://doi.org/10.1111/1467-8306.9302003

Washington, R., Todd, M.C. *et al*. 2006. Links between topography, wind, deflation, lakes and dust: the case of the Bodele Depression, Chad. *Geophysical Research Letters*, **33**, L09401, https://doi.org/10.1029/2006GL025827

Waters, C.N., Waters, R.A., Barclay, W.J. and Davies, J.R. 2009. *A lithostratigraphical framework for the Carboniferous successions of southern Great Britain (Onshore)*. British Geological Survey Research Report, **RR/09/01**.

Wentworth, C.K. 1922. A scale of grade and class terms for clastic sediments. *The Journal of Geology*, **30**.

Whalley, W.B., Smith, B.J., McAlister, J.J. and Edwards, A.J. 1987. Aeolian abrasion of quartz particles and the production of silt-size fragments: preliminary results. *Geological Society of America Special Publication*, **35**, 129–138, https://doi.org/10.1144/GSL.SP.1987.035.01.09

Wilkins, A.D., Hurst, A., Wilson, M.J. and Archer, S. 2018. Palaeo-environment in an ancient low-latitude, arid lacustrine basin with loessite: the Smith Bank Formation (Early Triassic) in the Central North Sea, UK Continental Shelf. *Sedimentology*, **65**, 335–359, https://doi.org/10.1111/sed.12382

Wilson, M.J., Hurst, A., Wilkins, A.D., Wilson, L. and Bowen, L. 2019. Mineralogical evidence for multiple dust sources in an early Triassic loessite. *Sedimentology*, **67**, 239–260, https://doi.org/10.1111/sed.12641

Wright, J. 2001. 'Desert' loess v. 'glacial' loess: quartz silt formation, source areas and sediment pathways in the formation of loess deposits. *Geomorphology*, **36**, 231–256, https://doi.org/10.1016/S0169-555X(00)00060-X

Wright, J., Smith, B. and Whalley, B. 1998. Mechanisms of loess-sized quartz silt production and their relative effectiveness: laboratory simulations. *Geomorphology*, **23**, 15–34, https://doi.org/10.1016/S0169-555X(97)00084-6

Yaalon, D.H. and Ganor, E. 1973. The influence of dust on soils in the Quaternary. *Soil Science*, **116**, 146–155, https://doi.org/10.1097/00010694-197309000-00003

Yamada, K. 2004. Last 40 ka climate changes as deduced from the lacustrine sediments of Lake Biwa, central Japan. *Quaternary International*, **123–125**, 43–50, https://doi.org/10.1016/j.quaint.2004.02.007

Yang, Y., Mason, J.A., Zhang, H., Lu, H., Ji, J., Chen, J. and Liu, L. 2017. Provenance of loess in the central Great Plains, USA based on Nd–Sr isotopic composition, and paleoenvironmental implications. *Quaternary Science Reviews*, **173**, 114–123, https://doi.org/10.1016/j.quascirev.2017.08.009

Ye, H., Royden, L., Burchfiel, C. and Schuepbach, M. 1996. Late Paleozoic deformation of interior North America: the greater Ancestral Rocky Mountains. *American Association of Petroleum Geologists Bulletin*, **80**, 1397–1432.

Yonkee, W.A., Dehler, C.D. *et al*. 2014. Tectono-stratigraphic frameworks of Neoproterozoic to Cambrian strata, west-central US: protracted rifting, glaciation, and evolution of the North American Cordilleran margin. *Earth-Science Reviews*, **136**, 59–95, https://doi.org/10.1016/j.earscirev.2014.05.004

Yoshioka, M., Mahowald, N.M., Conley, A.J., Collins, W.D., Fillmore, D.W., Zender, C.S. and Coleman, D.B. 2007. Impact of desert dust radiative forcing on sahel precipitation: relative importance of dust compared to sea surface temperature variations, vegetation changes, and greenhouse gas warming. *Journal of Climate*, **20**, 1445–1467, https://doi.org/10.1175/JCLI4056.1

Young, A., Flament, N., Williams, S.E., Merdith, A., Cao, X. and Müller, R.D. 2022. Long-term Phanerozoic sea level change from solid earth processes. *Earth and*

Planetary Science Letters, **584**, 117451, https://doi.org/10.1016/j.epsl.2022.117451

Zárate, M.A. 2003. Loess of southern South America. *Quaternary Science Reviews*, **22**, 1987–2006, https://doi.org/10.1016/S0277-3791(03)00165-3

Zeeden, C., Hambach, U. and Händel, M. 2015. Loess magnetic fabric of the Krems-Wachtberg archaeological site. *Quaternary International*, **372**, 188–194, https://doi.org/10.1016/j.quaint.2014.11.001

Zhu, R., Liu, Q. and Jackson, M.J. 2004. Paleoenvironmental significance of the magnetic fabrics in Chinese loess-paleosol since the last interglacial (<130 ka). *Earth and Planetary Science Letters*, **221**, 55–69, https://doi.org/10.1016/S0012-821X(04)00103-7